# Crustal Deformation Caused by the Yellowstone Uplift Detected by Anisotropic Receiver Functions

Mary Chen

Advisor: Jeffrey Park
Second Reader: Maureen Long

Department of Earth and Planetary Sciences
Yale University

A Senior Thesis presented to the faculty of the Department of Earth and Planetary Sciences, Yale University, in partial fulfillment of the Bachelor’s Degree.

Table of Contents

## Abstract

The Yellowstone hotspot is disrupting the stable crust of the North American Craton, beyond the immediate reach of its magmatism. The hotspot thermal anomaly uplifts the crust and creates a low-velocity partial melt layer in the middle crust. Tomographic imaging shows that its crustal magma reservoir extends well beyond the Yellowstone caldera with a size 2.5X that of previously imaged (Farrell et al. 2014). However, deformation in the shallow crust cannot be adequately detected with tomography. We estimate back-azimuth harmonics from receiver functions to detect for deformation throughout the crust (Park and Levin 2016). Using teleseismic data from long-standing stations of the Advanced National Seismic System (ANSS) and Global Seismographic Network (GSN), we investigate the anisotropic layering in the Yellowstone region. Seismic anisotropy expresses the azimuthal variations of seismic velocities and distorts wave polarizations and tractions to cause P waves to scatter to S waves with harmonic amplitude dependence. By estimating the harmonic amplitudes of P-to-S converted phases ('Ps scattering'), we can estimate the amount of anisotropy in the crust. The crust could be uniformly anisotropic, possess an anisotropic underplated layer, or develop shallow anisotropy from recent tectonic activity. Comparing the results from stations in and around Yellowstone, we discover greater anisotropic layering for stations found along the Yellowstone hotspot track than for stations near the Columbia River Basalt Group. Most stations that were untouched by the hotspot (e.g. HAWA) had modest anisotropic values. For example, there was strong anisotropic layering at shallow crustal depths (<15 km) beneath station RLMT (Red Lodge, Montana), which sits at the edge of the Yellowstone uplift. Strong two-lobed Ps amplitude variation at RLMT is consistent with tilted-axis anisotropy up to 21%. No ANSS stations in the undisturbed continental crust have a shallow-crust signal of that comparable amplitude.

## Introduction

The Pacific Northwest is home to one of the most complex geological formations: the Yellowstone hotspot. The Yellowstone Plateau propagated northeast following the eastern Snake River Plain (Christiansen, Foulger, and Evans 2002). Almost 17 million years ago, the Yellowstone hotspot track formed through a sequence of large volcanic calderas propagating northeast from the Oregon-Idaho-Nevada region, around the eastern Snake River Plain (Wicks et al. 2006; Yuan, Dueker, and Stachnik 2010). The caldera has been buried in rhyolite law flows around 150,000 to 70,000 years ago (Christiansen 2001). Today, the Yellowstone caldera lies within the Yellowstone Plateau. The Snake River Plain-Yellowstone volcanic system represents the propagating rift in Yellowstone. Earlier models suggested that the Yellowstone Plateau is at the tip of the rift. We now know that the volcanic field in the Yellowstone Plateau is the youngest section of the magmatic system (Christiansen, Fougler, Evans 2002).

This thesis builds a portfolio of modelled receiver functions to examine crustal anisotropy in the Yellowstone area by reviewing seismic stations in and around the Yellowstone hotspot track. We compare stations that are influenced by the hotspot versus those that are sited in undisturbed crust, untouched by the hotspot near the Columbia River basalts.

Located in the Pacific Northwest, the Columbia River Basalt Group formed around 17 million years ago from over 200,000 cubic kilometers of massive lava outpourings. The basaltic group is the best-preserved, youngest, and smallest continental flood basalt (Kasbohm and Schoene 2018). The Columbia basin includes Steens and Picture Gorge basalt formations.

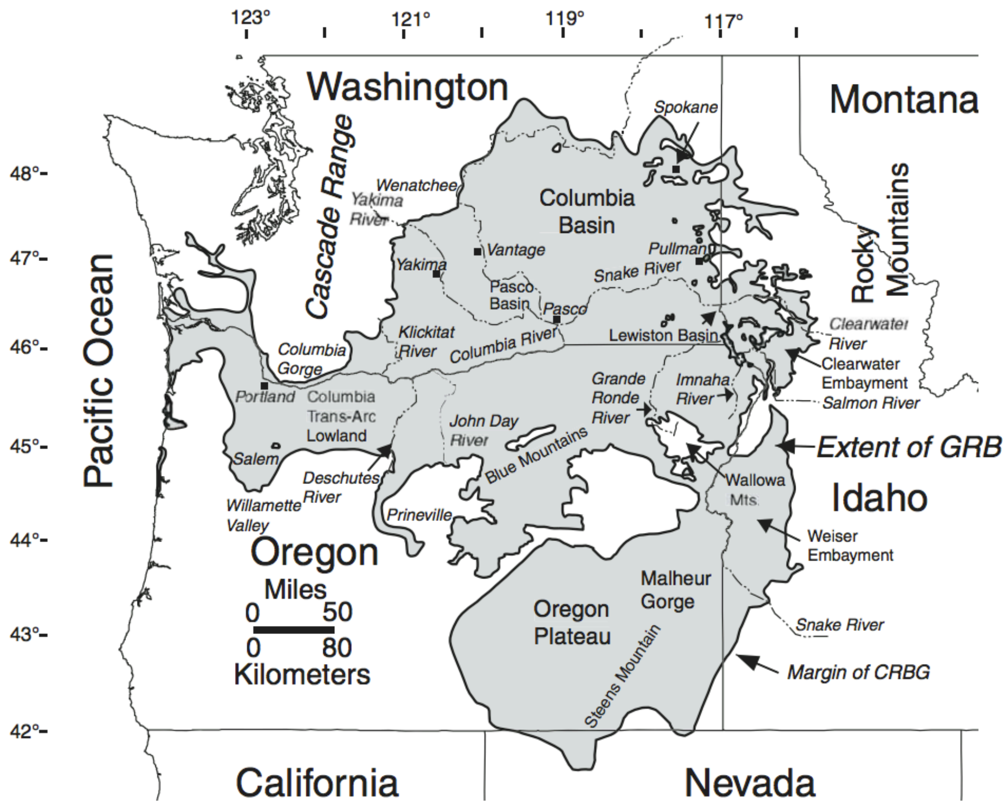


*Image 1: Map of the Columbia River Basalt Group. The Columbia River flood basalts exposures are in Washington, Oregon, Idaho and Nevada, USA. Source: Cascades Volcano Observatory, USGS.*

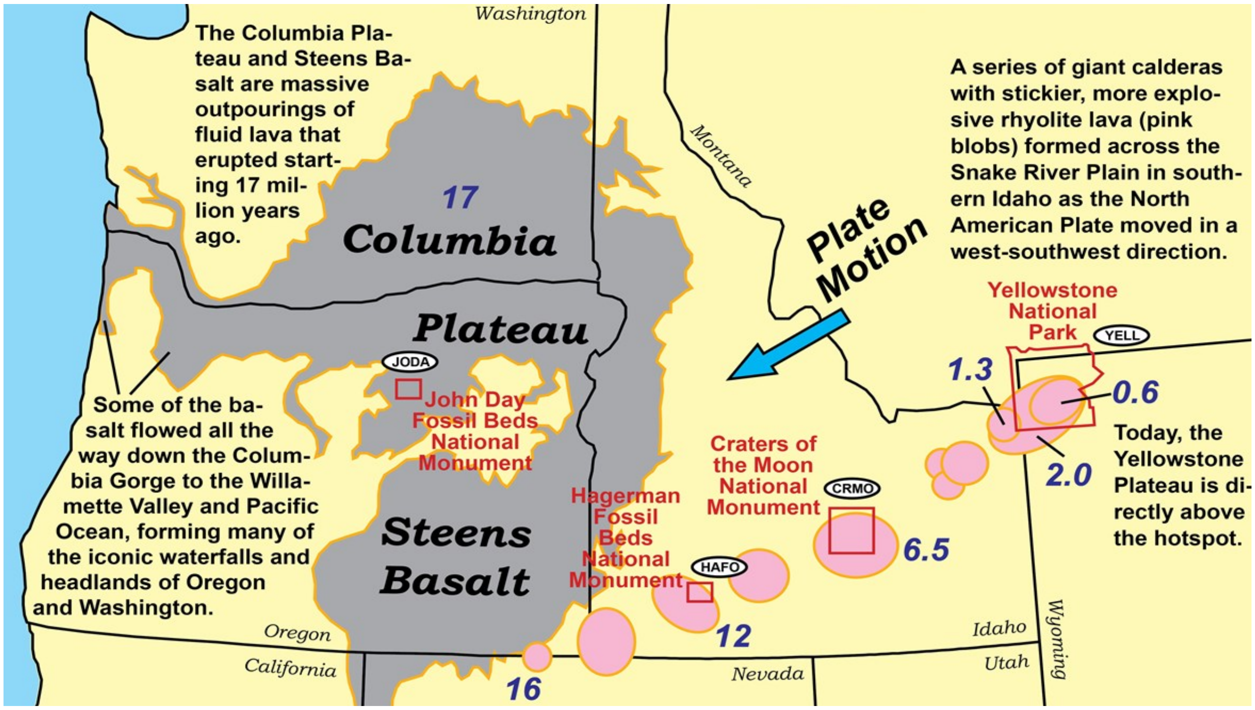


*Image 2: Map of the Pacific Northwest, USA including the Columbia River Basalt Group and the Yellowstone Hotspot Track. The pink circles indicate the calderas that have formed over several millions of years. The Yellowstone calderas have propagated northeast across the Snake River Plain as the North American Plate moves from the southwest. Source: USGS*

## Crustal Anisotropy

Seismic anisotropy measures the velocities of seismic waves to demonstrate the directional differences of an object. It occurs when rock properties such as texture or fabric, composition, and particle-size and shape distributions depend on direction, or when these properties interact with rock stress or temperature variations. Such anisotropy must be considered when using seismic waves to study subsurface structures, because the velocity of seismic waves can vary significantly depending on the direction that they propagate. Anisotropy can be found in the Earth's crust, mantle, and core. Specifically, crustal anisotropy produces P-to-SV and P-to-SH arrivals from P-to-S conversions along the Moho (Liu and Park 2017). By estimating the harmonic amplitudes of P-to-S converted phases ('Ps scattering'), the amount of anisotropy in the crust can be estimated.

The crust could be uniformly anisotropic, possess an anisotropic underplated layer, or develop shallow anisotropy from recent tectonic activity.

Levin and Park (1998) first demonstrated the effects of P and S anisotropy on converted seismic waves in a flat surface with anisotropy oriented in different ways. In their 1997 paper, Levin and Park explored the potential influence of crustal anisotropy on receiver functions using seismic station data from Russia around the Ural Mountains. Schulte-Pelkum and Mahan (2014) applied a novel approach to mapping crustal deformation using signals generated from inclined and anisotropic structures. They mapped the presence, the strike, and the depth of dipping of anisotropic structures in the continental United States. Frothingham et al (2022) attempted to map anisotropy onto the fault systems. Liu, Park, and Rye (2015) analyzed teleseismic data in Tibet to infer (sub)horizontal-axis crustal anisotropy. They argued that the mid-crustal shear is associated with a channel flow of viscous crust.

## Methods

We estimate back-azimuth harmonics from receiver functions to detect for deformation throughout the crust. Previous studies have applied tomographic imaging methods to understanding the Yellowstone hotspot more generally. Through tomographic imaging of the P wave velocity structure in Yellowstone, Farrell et al (2014) discovered that a large and low P-wave velocity body has fueled Yellowstone's volcanism. They found that the crustal magma reservoir is 2.5 times larger than what was previously imaged, with dimensions of 90 km long and between 5 to 17 km deep. However, deformation in the shallow crust cannot be adequately detected with tomography as tomography is not able to penetrate very deeply into the Earth's crust. Tomography is better suited for the mantle. Thus, our method of anisotropic receiver functions will provide a clearer narrative of the differences between the Yellowstone uplift and undisturbed crust.

Additionally, previous studies have been limited by crustal radial anisotropy for regions with particularly thick crust (Moschetti et al. 2010). However, in Yellowstone, we are looking at shallower crustal depths.

To build the dataset, I first selected the stations around and in Yellowstone that I wanted to investigate. I identified 20 seismic stations in and around the Yellowstone region and their respective station code and networks. The table below shows the 20 stations I originally began with. However, after issues related to the Jupyter Notebook and data retrieval process, I removed five of the stations. I did not finalize the data collection and compilation for the stations highlighted in yellow in the table below.[1] Ultimately, I collected and processed seismic data from 15 stations around Yellowstone from 2014 to 2019.

*Table 1: List of Seismic Stations (Name, Station Code, Latitude/Longitude, and Data Center)*

| Station Code | Station Name | Latitude | Longitude | Data Center(s) |
|---|---|---|---|---|
| AHID | Auburn Hatchery, Idaho, USA | 42.7654 | -111.1 | IRISDMC |
| BMN | Battle Mountain, Nevada, USA | 40.4315 | -117.22 | IRISDMC |
| BMO | Blue Mountains Array (Baker), Oregon, USA | 44.8525 | -117.31 | IRISDMC |
| BOZ | Bozeman, Montana, USA | 45.597 | -111.63 | IRISDMC |
| BW06 | Boulder Array Site 6 (Pinedale Array Site 6), Wyoming, USA | 42.7667 | -109.56 | IRISDMC |
| DGMT | Dagmar, Montana, USA | 48.4702 | -104.2 | IRISDMC |
| DUG | Dugway, Tooele County, Utah, USA | 40.195 | -112.81 | IRISDMC |
| EGMT | Eagleton, Montana, USA | 48.024 | -109.75 | IRISDMC |
| ELK | Elko, Nevada, USA | 40.7448 | -115.24 | IRISDMC / NCEDC |

[1] I could not collect any data for the BMN station (Battle Mountain, Nevada, US). I managed to collect only data from 2014 for the BW06 station (Boulder Array Site 6, Wyoming, US), but there was a change in seismometers, so data collection was limited. For the REDW station (Red Top Meadow, Wyoming, US), I only collected data from 2014 to 2016, but there was a change in networks, so I could not collect anymore data. For the RSSD and DGMT stations, I managed to collect all of the necessary data, but when I compiled it in the final Jupyter Notebooks that modelled the data to the receiver functions, the program did not work due to indexing issues.

| | | | | |
|---|---|---|---|---|
| HAWA | Hanford, Washington, USA | 46.3925 | -119.53 | IRISDMC |
| HLID | Hailey, Idaho, USA | 43.5625 | -114.41 | IRISDMC |
| HWUT | Hardware Ranch, Cache County, Utah, USA | 41.6069 | -111.57 | IRISDMC |
| LAO | LASA Array, Montana, USA | 46.6885 | -106.22 | IRISDMC |
| LKWY | Lake (Yellowstone--Lake), Yellowstone National Park, Wyoming | 44.5652 | -110.4 | IRISDMC |
| MSO | Missoula, Montana, USA | 46.8292 | -113.94 | IRISDMC |
| NEW | Newport, Washington, USA | 48.2642 | -117.12 | IRISDMC |
| REDW | Red Top Meadow, Wyoming, USA | 43.3624 | -110.85 | IRISDMC |
| RLMT | Red Lodge, Montana, USA | 45.1221 | -109.27 | IRISDMC |
| RSSD | Black Hills, South Dakota, USA | 44.1204 | -104.04 | IRISDMC |
| WVOR | Wild Horse Valley, Oregon, USA | 42.4339 | -118.64 | IRISDMC / NCEDC |

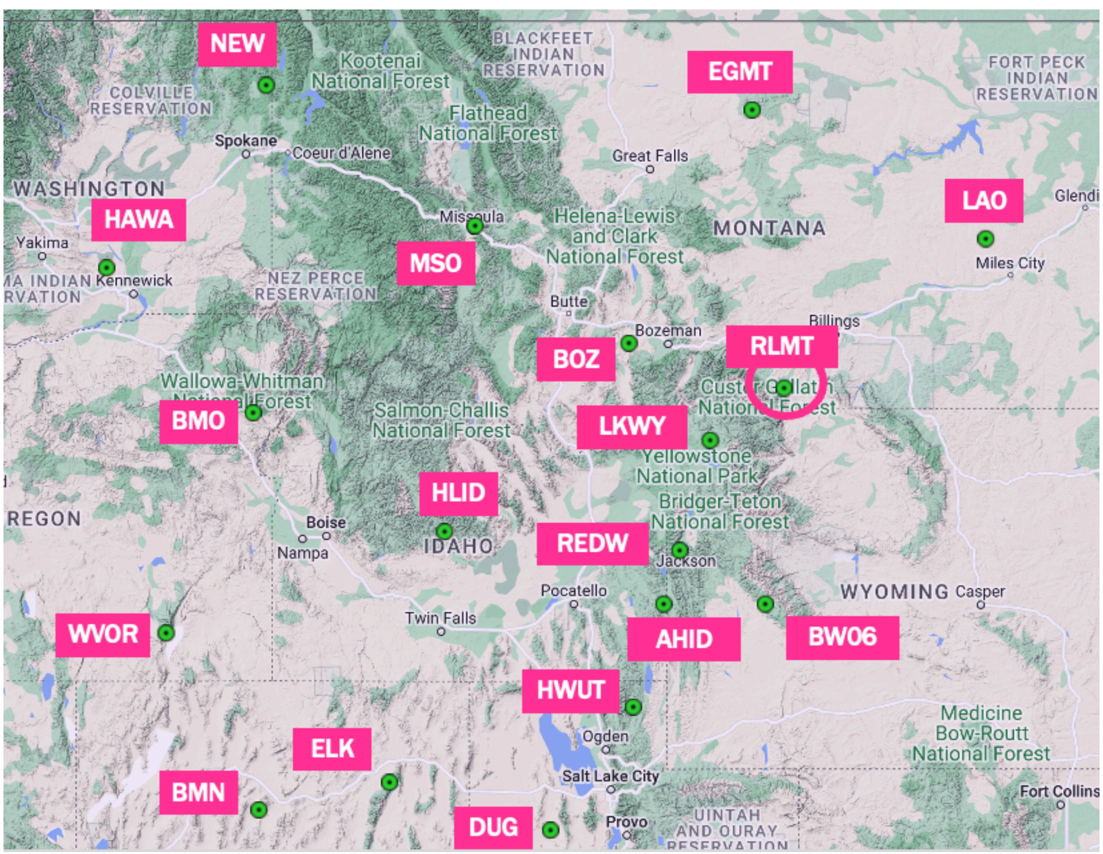


*Figure 1: Map of Seismic Stations around Yellowstone from IRIS. The circled station (RLMT) indicates where the Yellowstone Caldera is.*

Then, I used Jupyter Notebook running ObsPy, which is an open-source project for processing seismic data, for direct data retrieval from Incorporated Research Institutions for Seismology (IRIS). [2] For each station, there were two notebooks. The first notebook was designed specifically to retrieve the data for the year requested. I processed all the radial, transverse, and vertical components available for each long-standing station in the Advanced National Seismic System (ANSS) and Global Seismographic Network (GSN) for seismic events with a magnitude greater than 6. In order to ensure quality control of the dataset, I filtered the data through a low pass and high pass filtering to determine if there is a real signal. Below is an example of the quality control process step. I completed this process for all of my stations, and I saved over 8800 events.

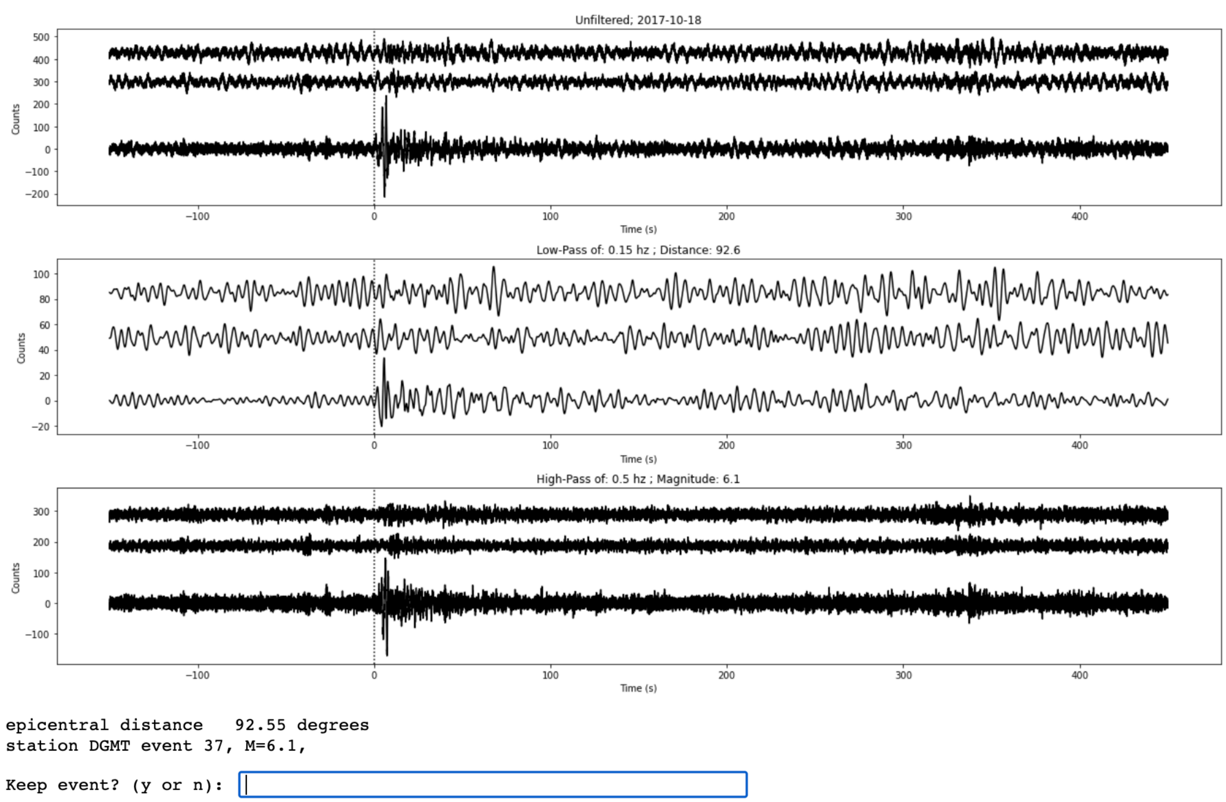


*Figure 2: This shows a seismograph for a potential event in Dagmar, Montana (DGMT). There are three plots of data: unfiltered, low-pass filtered, and high-pass filtered data. In each plot, there*

[2] Jeffrey Park and Will Frazer wrote the code in Python. I made minor edits according to the necessary stations we needed data from.

*are three components: radial, transverse, and vertical. The Jupyter Notebook only retrieves events with a magnitude greater than 6. The notebook allows the user to save ("y") or reject "n" the seismograph.*

The second notebook combined all the receiver functions across the six years' worth of data into one analysis for each station. The visualizations below are produced from the second notebook. For both Jupyter Notebooks, the code allowed the user to quality control check the seismic events for each station for the respective year, establish the back-azimuth range for the visualizations, and set the target depth. I selected a depth of 35km, which is roughly where the Mohorovičić Discontinuity (Moho Discontinuity) is. The back-azimuth range was 0 to 360.0.

The receiver function method has previously been used in prior studies (Eagar, Fouch, and James 2010; Park and Levin 2016; Schulte-Pelkum and Mahan 2014). Receiver functions are frequency domain estimates that are calculated through inverse Fourier transformations. The method "isolates teleseismic mode conversions originating at velocity contrasts beneath a seismic station" (Schulte-Pelkum and Mahan 2014).

## Results

*Auburn Hatchery, Idaho, USA (AHID)*

Start / End Date: 1997-11-12 / 2499-01-01

Elevation: 1960 m

Saved Events from 2014-2019: 544

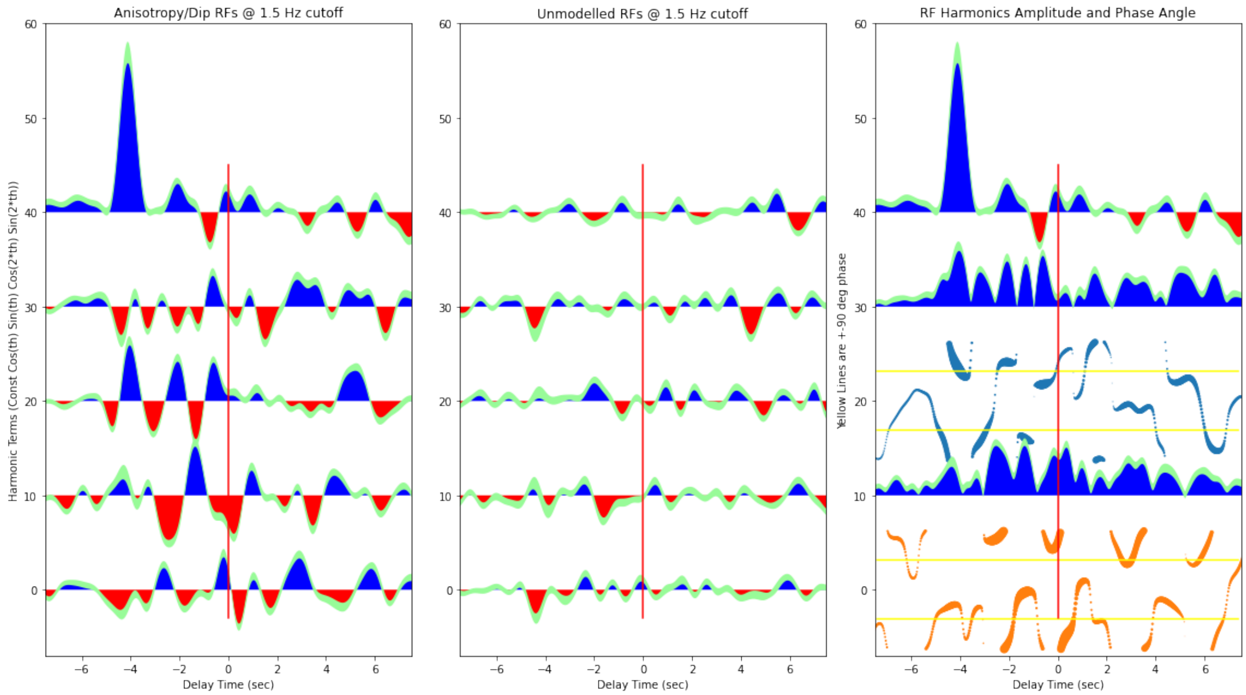


*Figure 3: The left panel is a plot of anisotropy and dip receiver functions at 1.5 Hz cutoff. The first graph in this panel is the constant plot that models the isotropic structure. The next two graphs are two-lobed plots of tilted axis anisotropy. The next two are four lobed amplitude variations modeling the horizontal anisotropy. The middle panel is the unmodelled receiver functions at 1.5 Hz cutoff. The right panel is the receiver functions harmonics amplitude and phase angle plot also at 1.5 Hz cutoff. The first plot is the constant model for the isotropic structure. The all-blue pulses are the result of the absolute value of the 2 lobed amplitude variations. The blue wisps plot the strike axis of symmetry. The next set of all-blue pulses are the absolute value of the 4 lobed amplitude variations. The orange wisps are the phase angle of the 4 lobe amplitude variations. The delay time at 0 seconds refers to the target depth, which is the Moho depth. We estimate that to be 35km. At the delay time of zero seconds in the modelled receiver functions, there is a blue pulse, suggesting the Moho for this location is around 35km. Note that there is another blue pulse following the zero seconds delay time. This could be a secondary Moho. There is tilted anisotropy throughout the crust of around 7% and horizontal anisotropy in the lower crust. There is a red pulse right before the target depth, suggest a low-velocity zone. The anisotropic orientation within some of layers are stable and facing the same direction.*

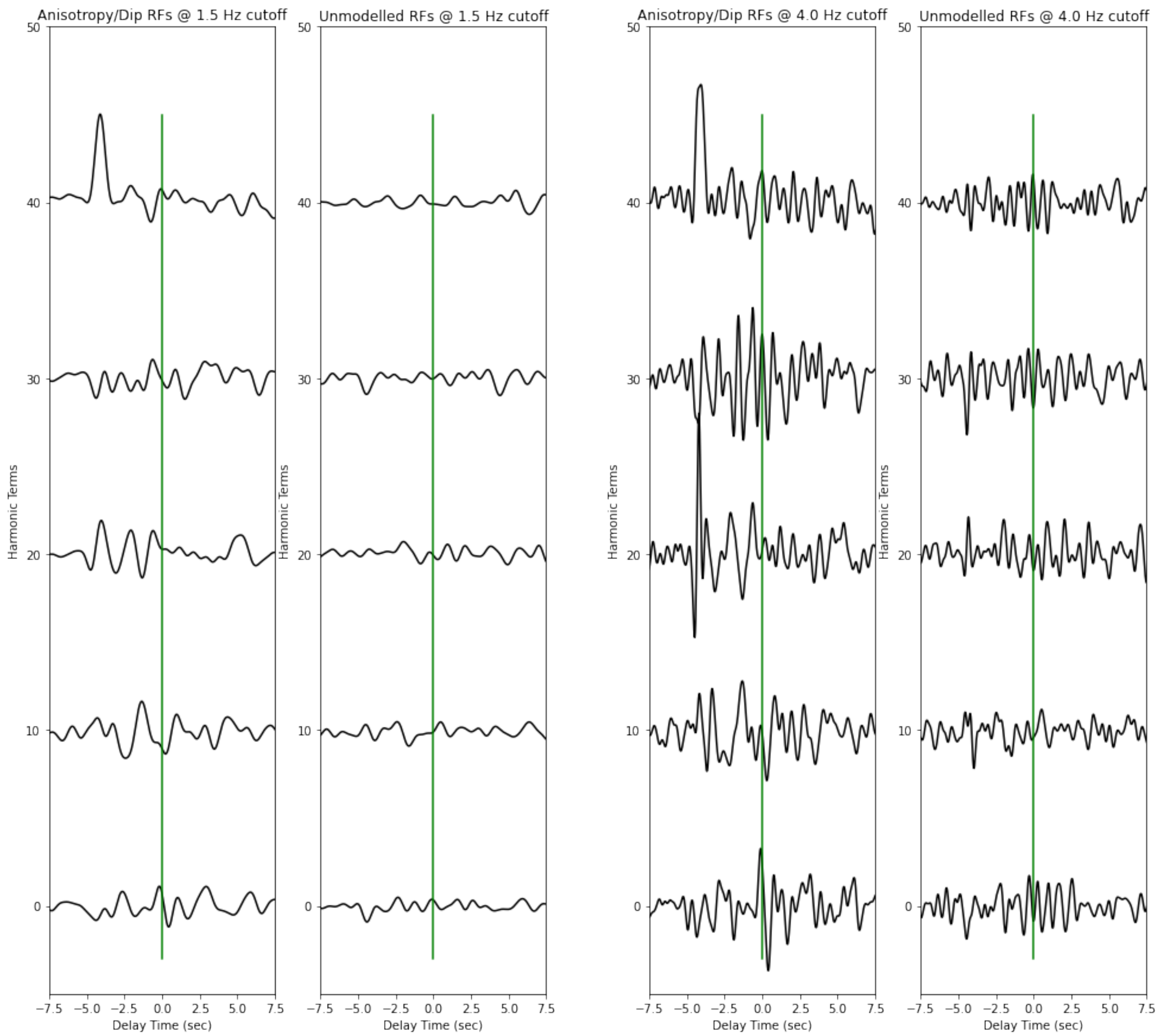


*Figure 4: This is the anisotropy receiver functions for two different frequency cutoffs (1.5 Hz and 4.0 Hz) for AHID. Both frequency cutoffs show the same features of high anisotropy in the lower crust. The higher frequency cutoff has higher unmodelled energy. Below are the minimum and maximum amplitude values for each respective plot: constant, two-lobed, and four-lobed. Tilted anisotropy is 1 to 11% and horizontal anisotropy is 1 to 3%.*

| | |
|---|---|
| cmin = -0.014714472485284078 | cmin = -0.027534644600084052 |
| cmax = 0.0669066797758101 | cmax = 0.08940019320366725 |
| 2min = -0.015761907597294015 | 2min = -0.046875841786264735 |
| 2max = 0.01429152535862728 | 2max = 0.053549459936988404 |
| 2min = -0.017876452549953296 | 2min = -0.06303311660057745 |
| 2max = 0.025558680637237426 | 2max = 0.10685482253762904 |
| 4min = -0.021262575791390435 | 4min = -0.03830273011479202 |
| 4max = 0.021792037270756345 | 4max = 0.037194244988009564 |
| 4min = -0.015810560237427742 | 4min = -0.04904430323202934 |
| 4max = 0.014893774658913882 | 4max = 0.04358724743803689 |

*Blue Mountains Array (Baker), Oregon, USA (BMO)*
Start / End Date: 2004-11-23 / 2499-01-01
Elevation: 1189 m
Saved Events from 2014-2019: 604

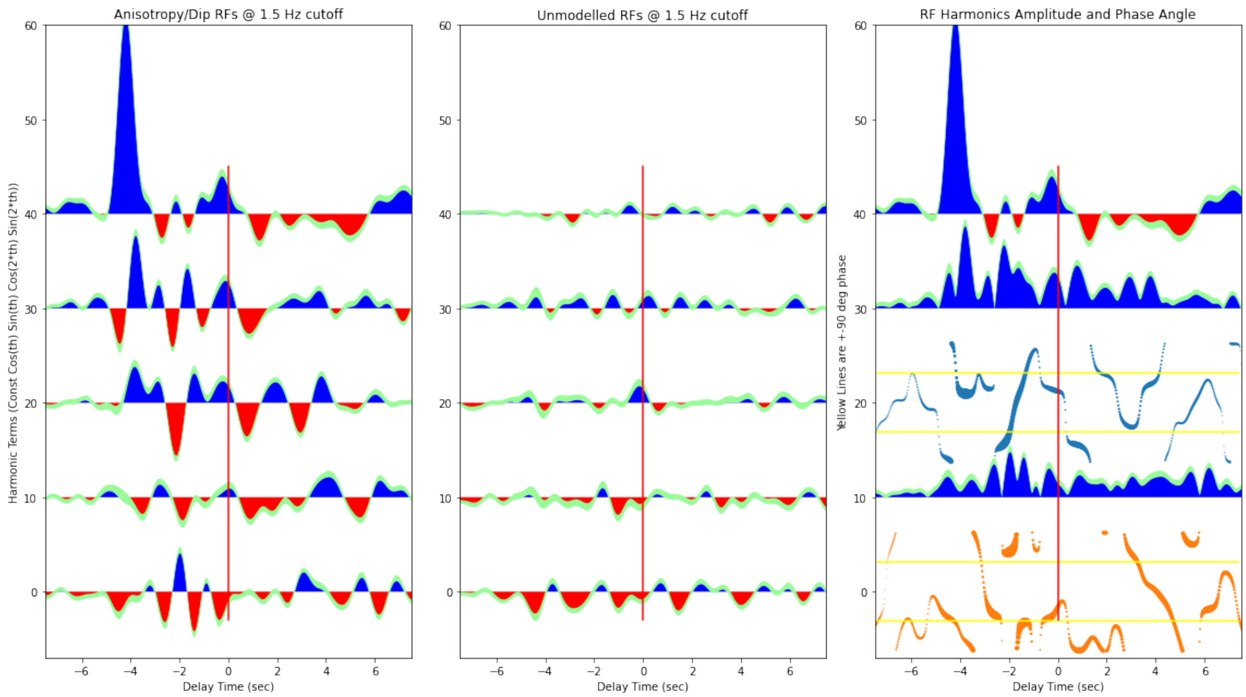


*Figure 5: Models of Anisotropy/Dip RFs, Unmodelled RFs, and RF Harmonics Amplitude and Phase Angle at 1.5 Hz cutoff Plots for BMO. The Moho appears to be around 35 km as indicated by the blue pulse at the 0 sec delay time. There is tilted anisotropy and horizontal anisotropy throughout the lower crust. There are several red pulses under the Moho, suggesting there may be a hot mantle as denoted by the low velocities. The anisotropic orientation within some of the layers before the Moho are not stable and facing the same direction.*

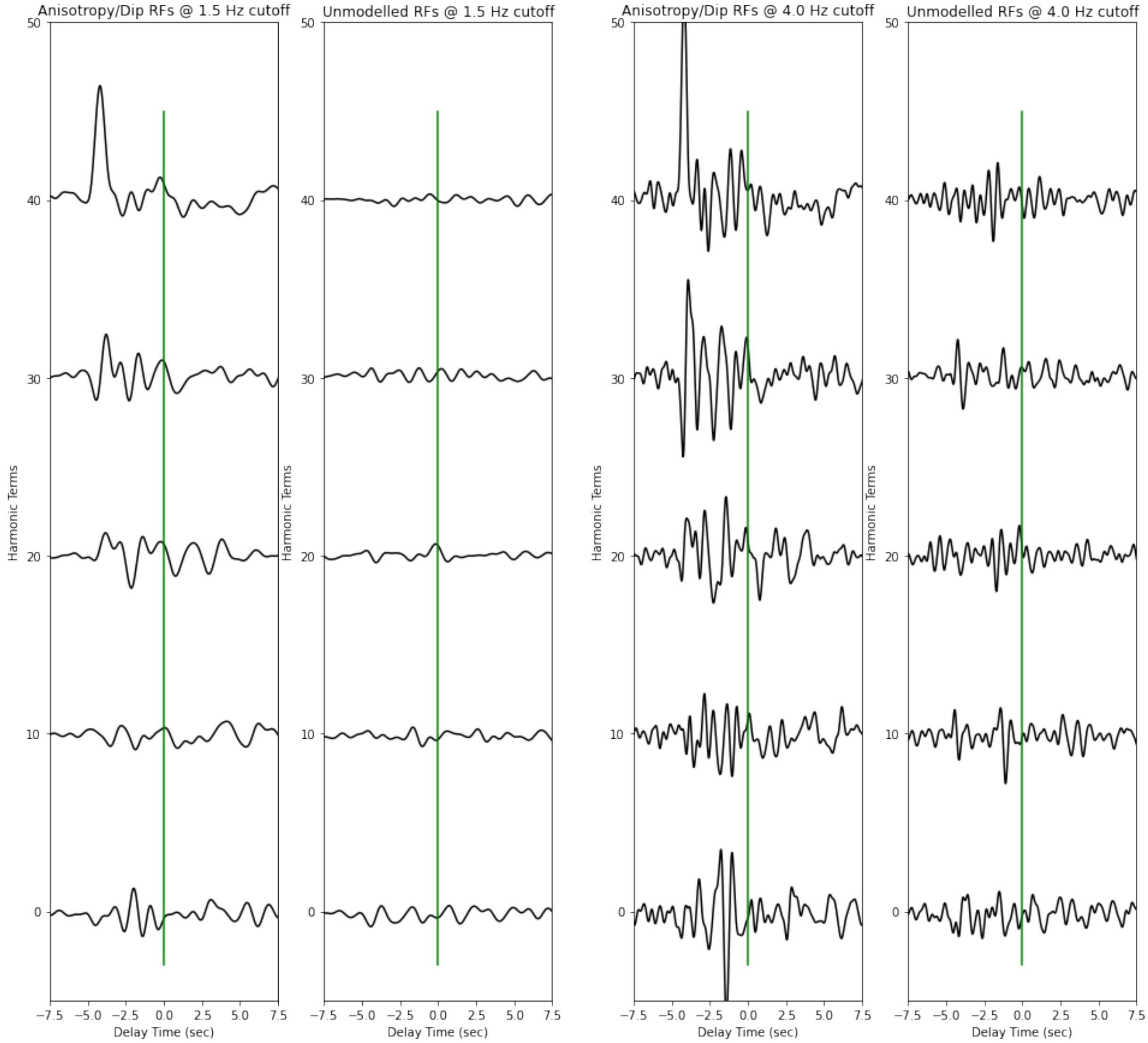


*Figure 6: Modelled and Unmodelled Receiver Functions for 1.5 and 4.0 Hz cutoffs for BMO. There is tilted and horizontal anisotropy of around 1 to 4%. BMO is located outside of the Yellowstone hotspot track, near the Columbia River basalts, so it makes sense that BMO would have modest anisotropy values.*

| | |
|---|---|
| cmin = -0.012726327917979887 | cmin = -0.038357302854215965 |
| cmax = 0.08569619512260356 | cmax = 0.16060574337058467 |
| 2min = -0.017113291217805377 | 2min = -0.059220566328253205 |
| 2max = 0.03265305498556399 | 2max = 0.07358588333307467 |
| 2min = -0.024174938431438687 | 2min = -0.03531762360745124 |
| 2max = 0.017208818472361775 | 2max = 0.044166337988457156 |
| 4min = -0.011909800938881745 | 4min = -0.03194429977415496 |
| 4max = 0.009216178650499464 | 4max = 0.029911476714153968 |
| 4min = -0.018734224767776805 | 4min = -0.08139282785668045 |
| 4max = 0.017386656569078007 | 4max = 0.04645389078669773 |

*Bozeman, Montana, USA (BOZ)*
Start / End Date: 1999-11-11 / 2499-01-01
Elevation: 1589 m
Saved Events from 2014-2019: 567

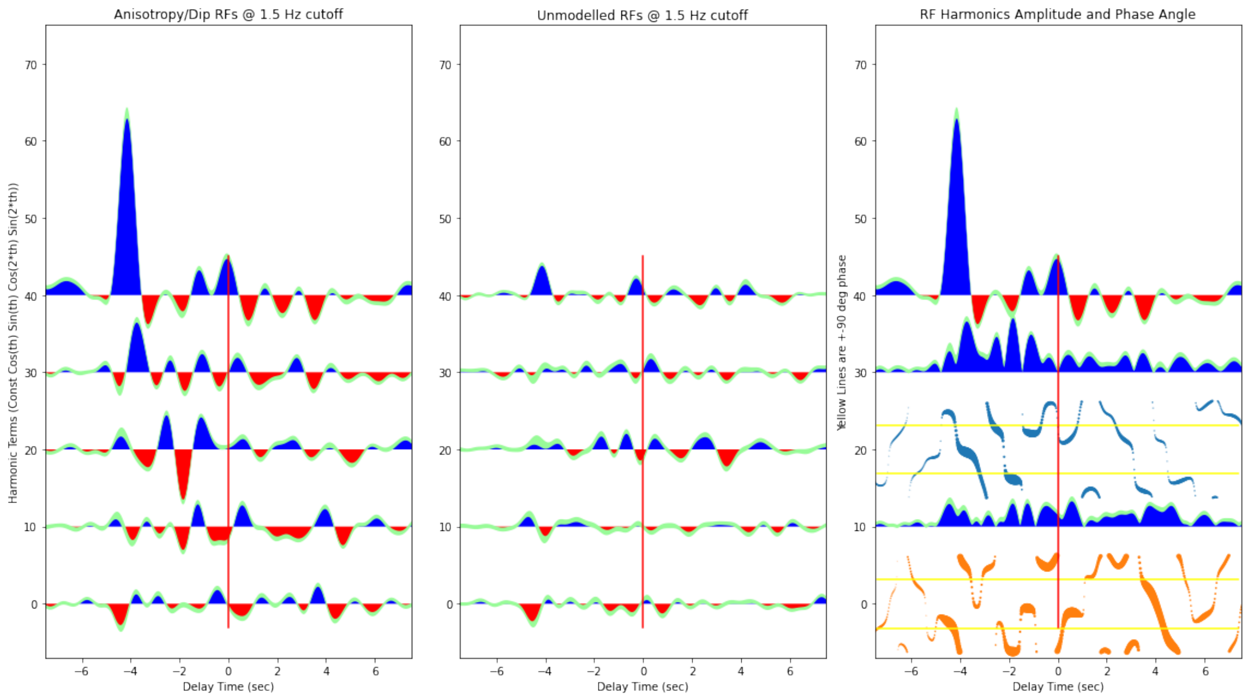


*Figure 7: Models of Anisotropy/Dip RFs, Unmodelled RFs, and RF Harmonics Amplitude and Phase Angle at 1.5 Hz cutoff Plots for BOZ. The Moho appears to be around 35 km as indicated by the blue pulse at the 0 sec delay time. There is tilted anisotropy and horizontal anisotropy throughout the lower crust. The anisotropic orientation within some of the layers are stable and facing the same direction.*

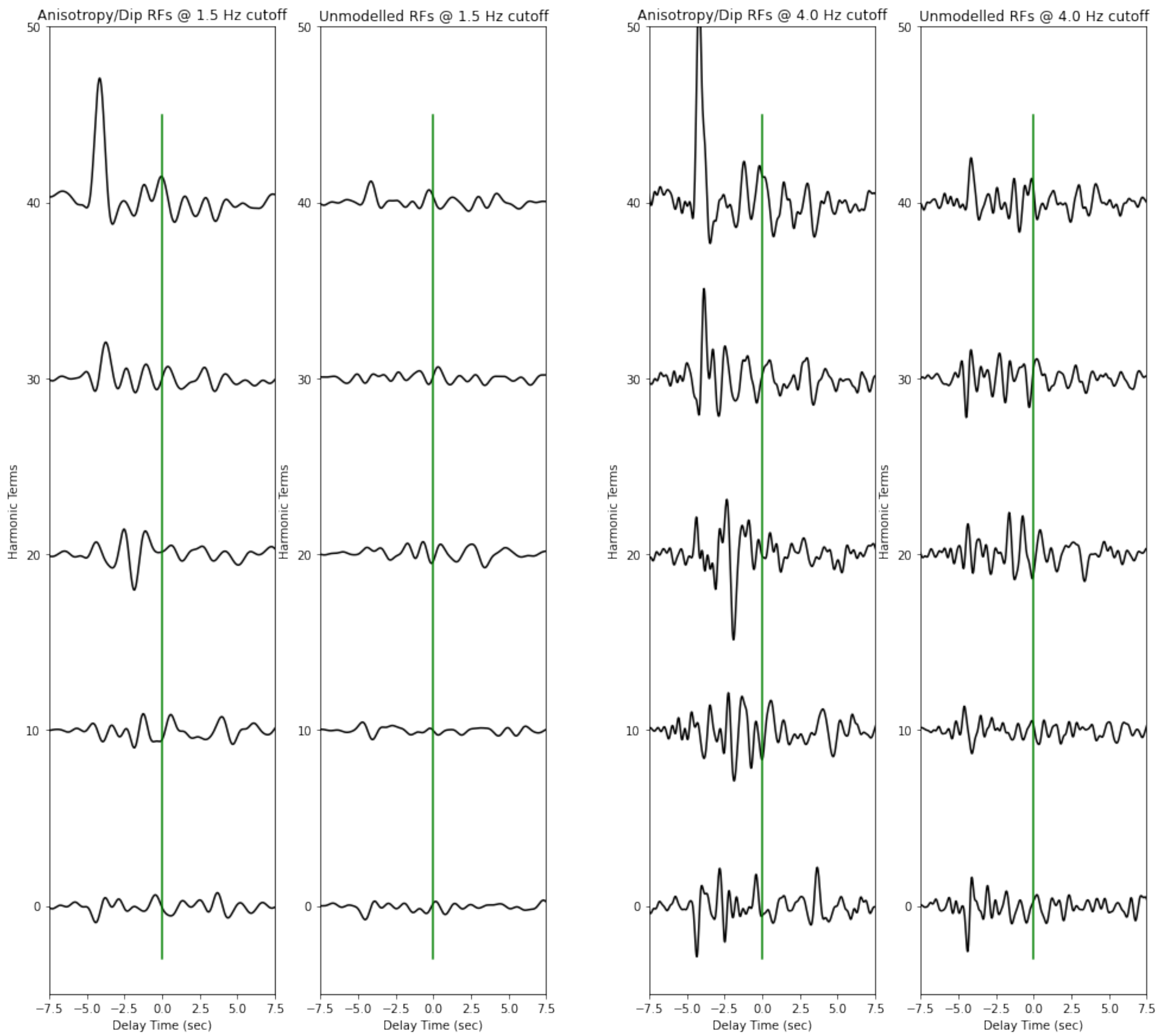


*Figure 8: Modelled and Unmodelled Receiver Functions for 1.5 and 4.0 Hz cutoffs for BOZ. There is tilted and horizontal anisotropy of around 1 to 4%. BOZ is found slightly outside of Yellowstone (west), so it makes sense that the anisotropic values are modest.*

cmin = -0.016405618774395444
cmax = 0.09420798677881431
2min = -0.010825717228674507
2max = 0.027375477766968883
2min = -0.0271131562105455
2max = 0.019016989563698152
4min = -0.013396982544120603
4max = 0.012392178551318061
4min = -0.012549567730320304
4max = 0.010059712908943702

cmin = -0.031046806304508286
cmax = 0.1682745242054812
2min = -0.028634735237103873
2max = 0.06796161488534926
2min = -0.0648770702634971
2max = 0.04152671439006815
4min = -0.03845854931185094
4max = 0.02827483128252429
4min = -0.03845621147782867
4max = 0.029305039485332963

*Boulder Array Site 6 (Pinedale Array Site 6), Wyoming, USA (BW06)*
Start / End Date: 1996-05-05 / 2499-01-01
Elevation: 2224 m
Saved Events (2014): 102

For this station, I could only download data from 2014 because there was a change in networks, which resulted in me saving 102 events.

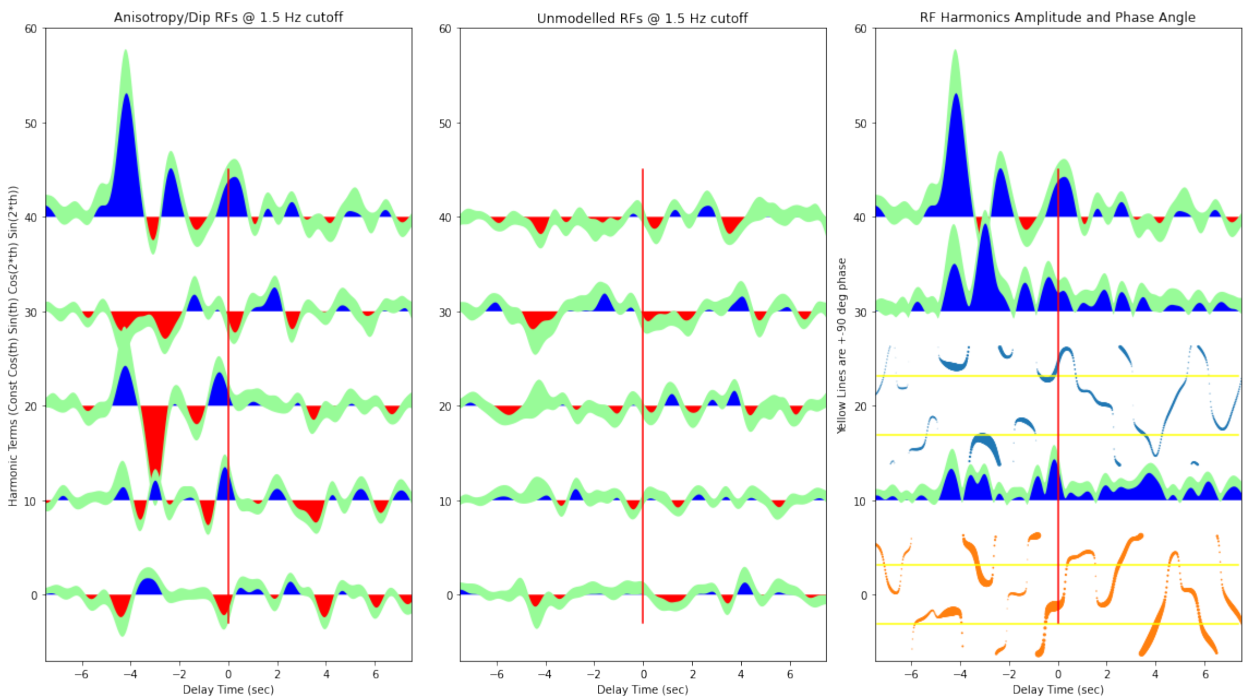


*Figure 9: Models of Anisotropy/Dip RFs, Unmodelled RFs, and RF Harmonics Amplitude and Phase Angle at 1.5 Hz cutoff Plots for BW06. The Moho appears to be around 35 km as indicated by the blue pulse at the 0 sec delay time. There is tilted anisotropy and horizontal anisotropy throughout the lower crust. Note that the uncertainties, which are calculated by bootstrapping, are much greater because there was not enough data compared to other stations. The anisotropic orientation within some of the layers are stable but not facing the same direction.*

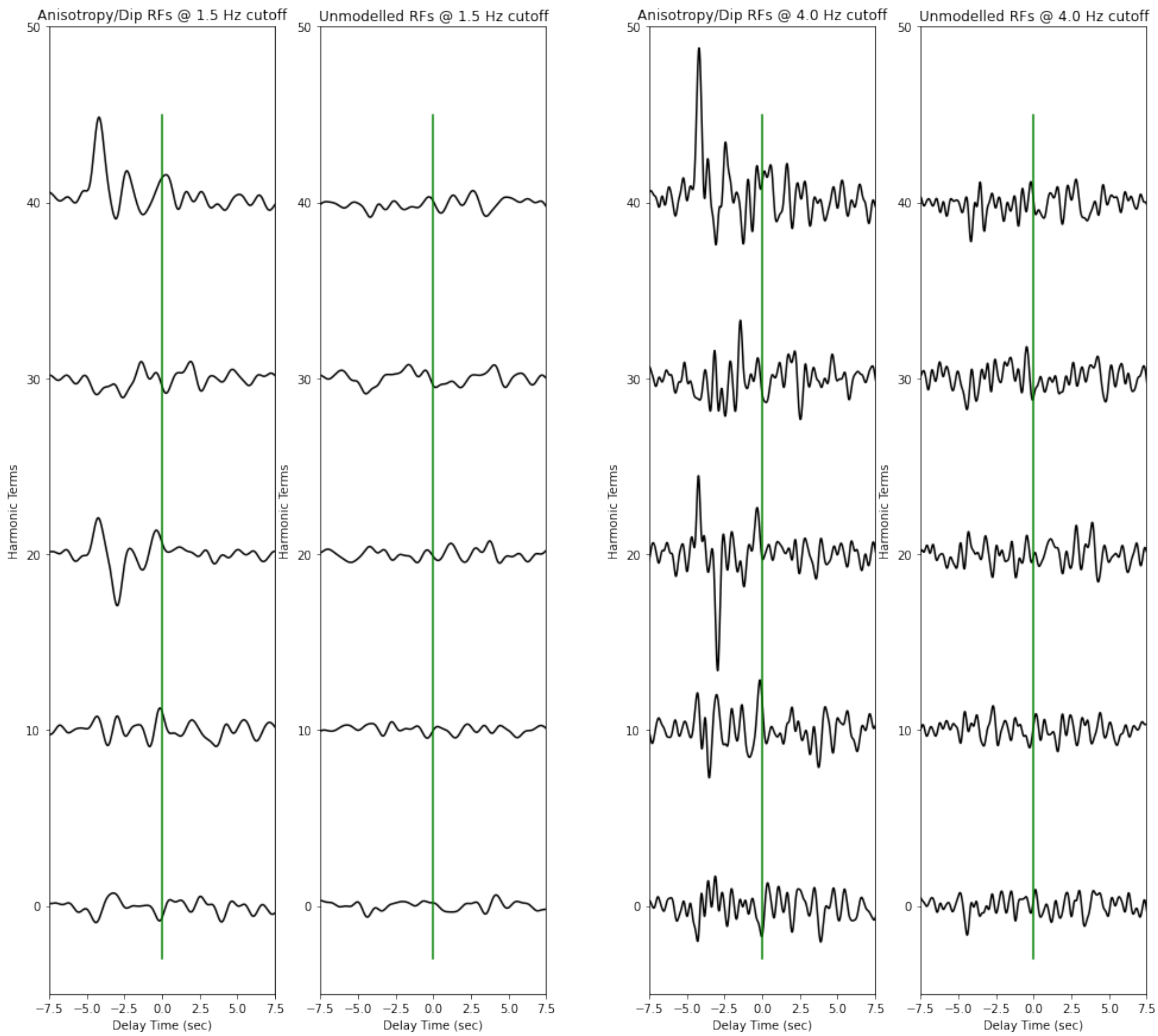


*Figure 10: Modelled and Unmodelled Receiver Functions for 1.5 and 4.0 Hz cutoffs for BW06. There is tilted anisotropy of around 1 to 6%. There is horizontal anisotropy of around 1 to 3% BW06 is found east of the hotspot track, so anisotropic values are slightly higher compared to that of BOZ as the hotspot is propagating northeast.*

| | |
|---|---|
| cmin = -0.012390702148476764 | cmin = -0.03207595753023653 |
| cmax = 0.06461889033568835 | cmax = 0.11702313699374375 |
| 2min = -0.014619707474968205 | 2min = -0.031193249428926543 |
| 2max = 0.012793786524268226 | 2max = 0.04400008698394814 |
| 2min = -0.038985448869274186 | 2min = -0.0882351953884304 |
| 2max = 0.027586885298928533 | 2max = 0.05951009292253535 4 |
| 4min = -0.012435176908221891 | 4min = -0.0361385533798094 |
| 4max = 0.01671907793472231 | 4max = 0.038025116464335644 |
| 4min = -0.01253838347068735 | 4min = -0.027266379659971283 |
| 4max = 0.00980063307210134 | 4max = 0.02256369127586452 |

Prior to 2013, could not get enough data (only saved 5 events), so this is what I saw for 2013, where the waveforms are completely unreadable.

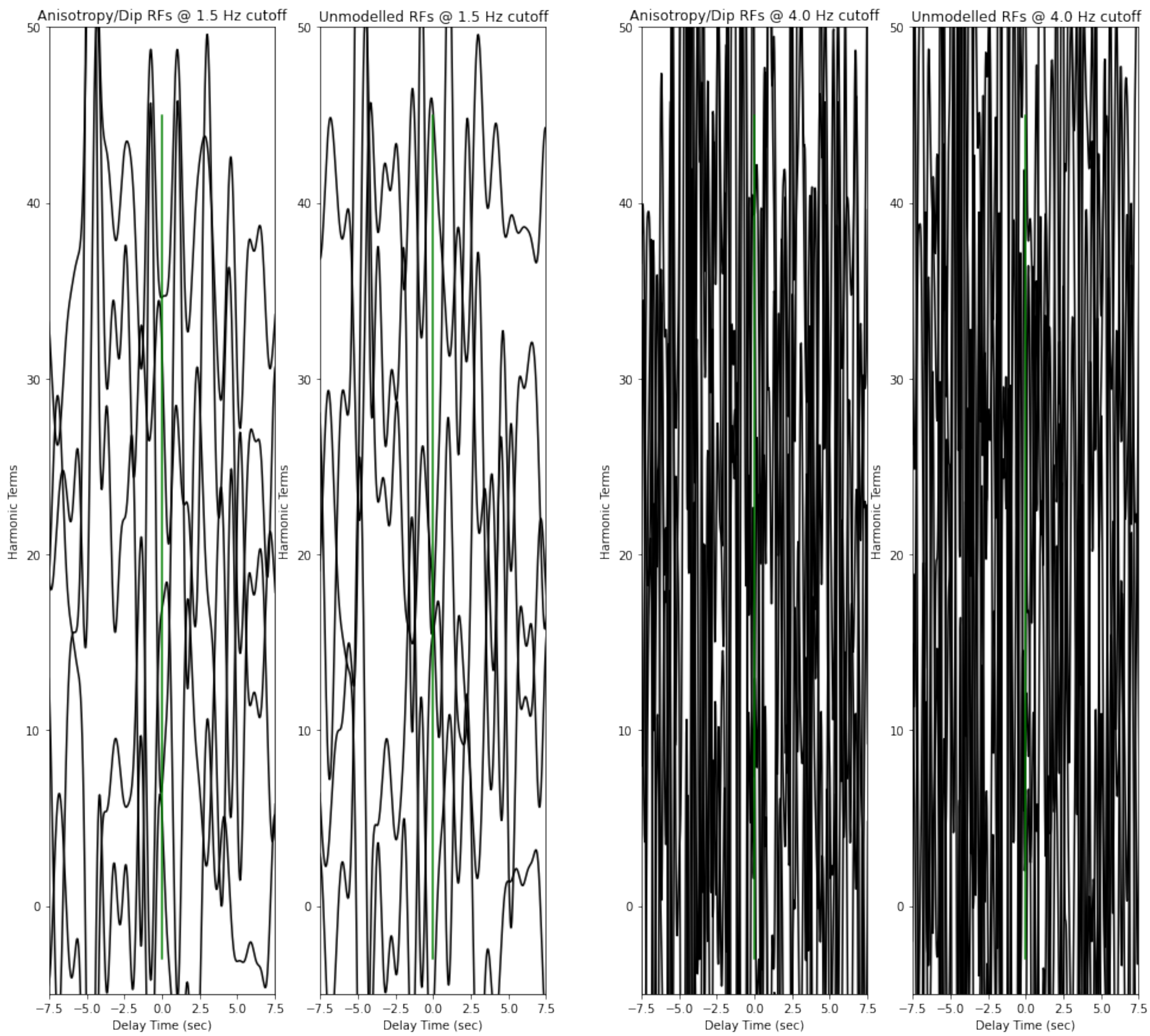


*Figure 11: Modelled and Unmodelled Receiver Functions for 1.5 and 4.0 Hz cutoffs for BW06. Results are inconclusive for 2013 data.*

*Dugway, Tooele County, Utah, USA (DUG)*
Start / End Date: 1993-02-18 / 2499-01-01
Elevation: 1477 m
Saved Events from 2014-2019: 580

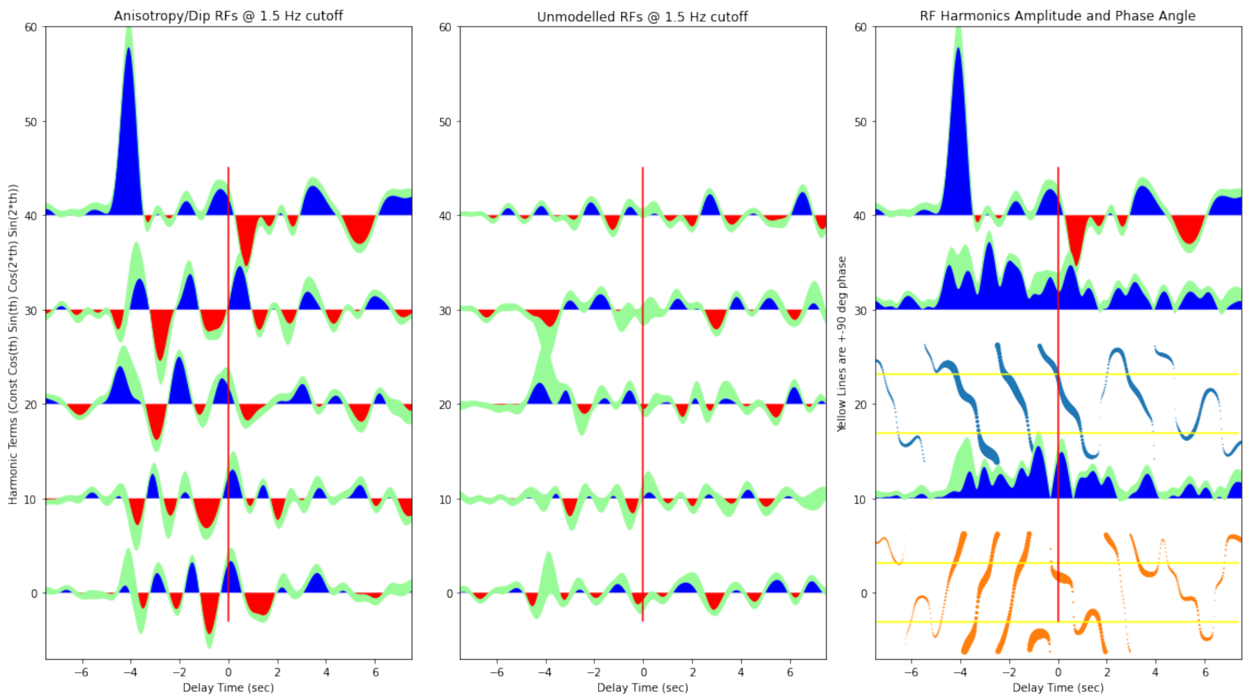


*Figure 12: Models of Anisotropy/Dip RFs, Unmodelled RFs, and RF Harmonics Amplitude and Phase Angle at 1.5 Hz cutoff Plots for DUG. The Moho appears to be around 35 km as indicated by the blue pulse at the 0 sec delay time. It may be a little shallower than 35 km. There is tilted anisotropy and horizontal anisotropy throughout the lower crust. There are several red pulses under the Moho, suggesting there may be a hot mantle as denoted by the low velocities. The anisotropic orientation within some of the layers are stable but are facing the same direction. Additionally, there is significant twisting in the lower crust.*

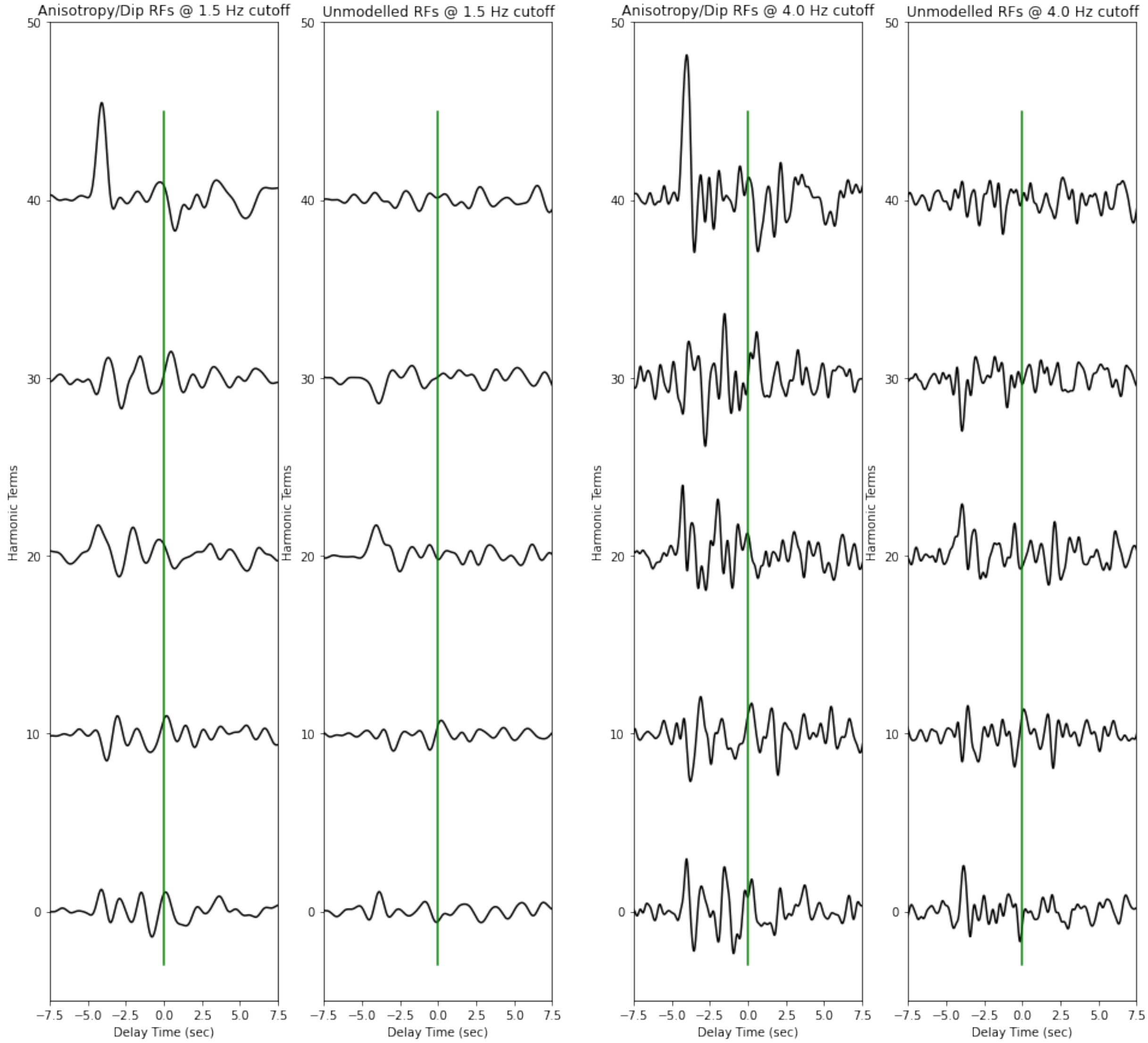


*Figure 13: Modelled and Unmodelled Receiver Functions for 1.5 and 4.0 Hz cutoffs for DUG. There is tilted anisotropy of around 2 to 5%. There is horizontal anisotropy of about 1 to 3%. DUG away from the hotspot track in northwestern Utah, so anisotropic values will be modest.*

cmin = -0.02314886406772926
cmax = 0.07297705557733322
2min = -0.023060373667404127
2max = 0.019811728579837373
2min = -0.0156870494610519
2max = 0.023070973839909827
4min = -0.020327385382191986
4max = 0.01337515399942333
4min = -0.019011814047058782
4max = 0.016526320394448242

cmin = -0.0391676939107455
cmax = 0.10868131111506613
2min = -0.05119465584737024
2max = 0.04812123113005173
2min = -0.025784824593618704
2max = 0.052825982873694007
4min = -0.03579223073313802
4max = 0.027693695511286722
4min = -0.03144940430301257
4max = 0.039450583620722394

*Eagleton, Montana, USA (EGMT)*

Start / End Date: 2005-11-17 / 2499-01-01

Start / End Date: 2005-10-01 / 2999-12-31

Elevation: 1055 m

Saved Events from 2014-2019: 589

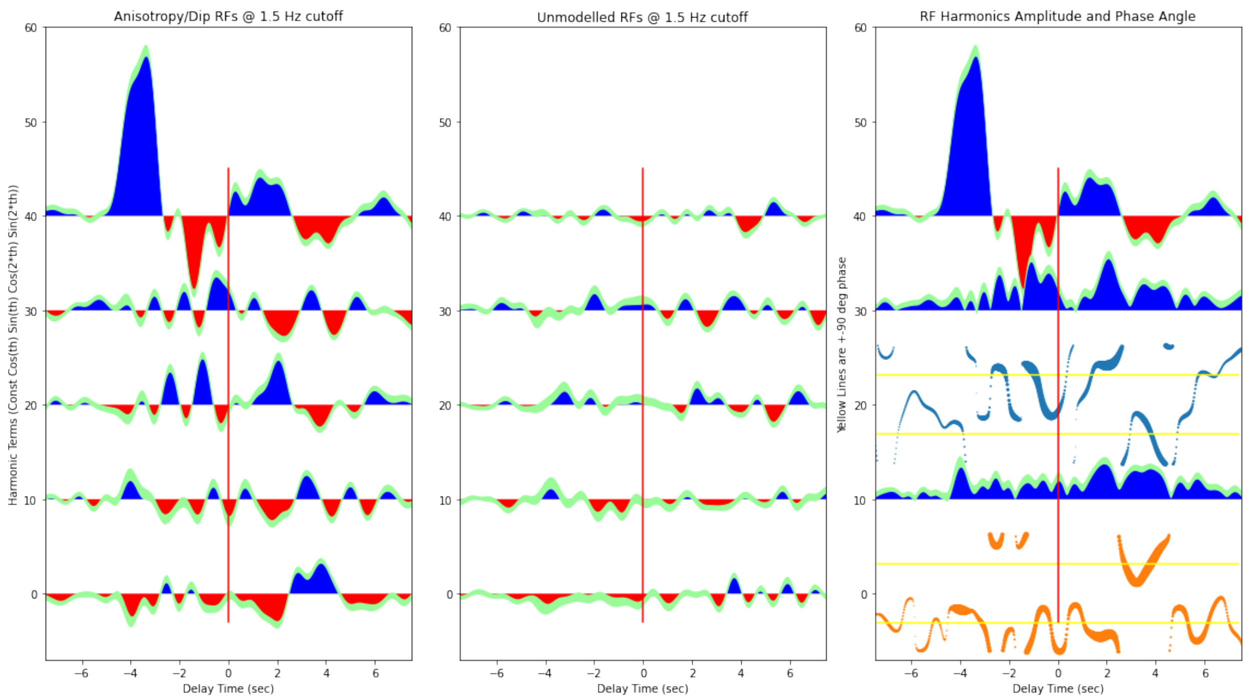


*Figure 14: Models of Anisotropy/Dip RFs, Unmodelled RFs, and RF Harmonics Amplitude and Phase Angle at 1.5 Hz cutoff Plots for EGMT. The location of the Moho is uncertain. It could be a little deeper than 35 km (the blue pulse after the 0 sec delay time), but the Moho could also be around -3 and -4 sec (the first large blue pulse). There is tilted anisotropy and horizontal anisotropy throughout the lower crust. The anisotropic orientation within some of the layers are stable near the target depth but facing the same direction.*

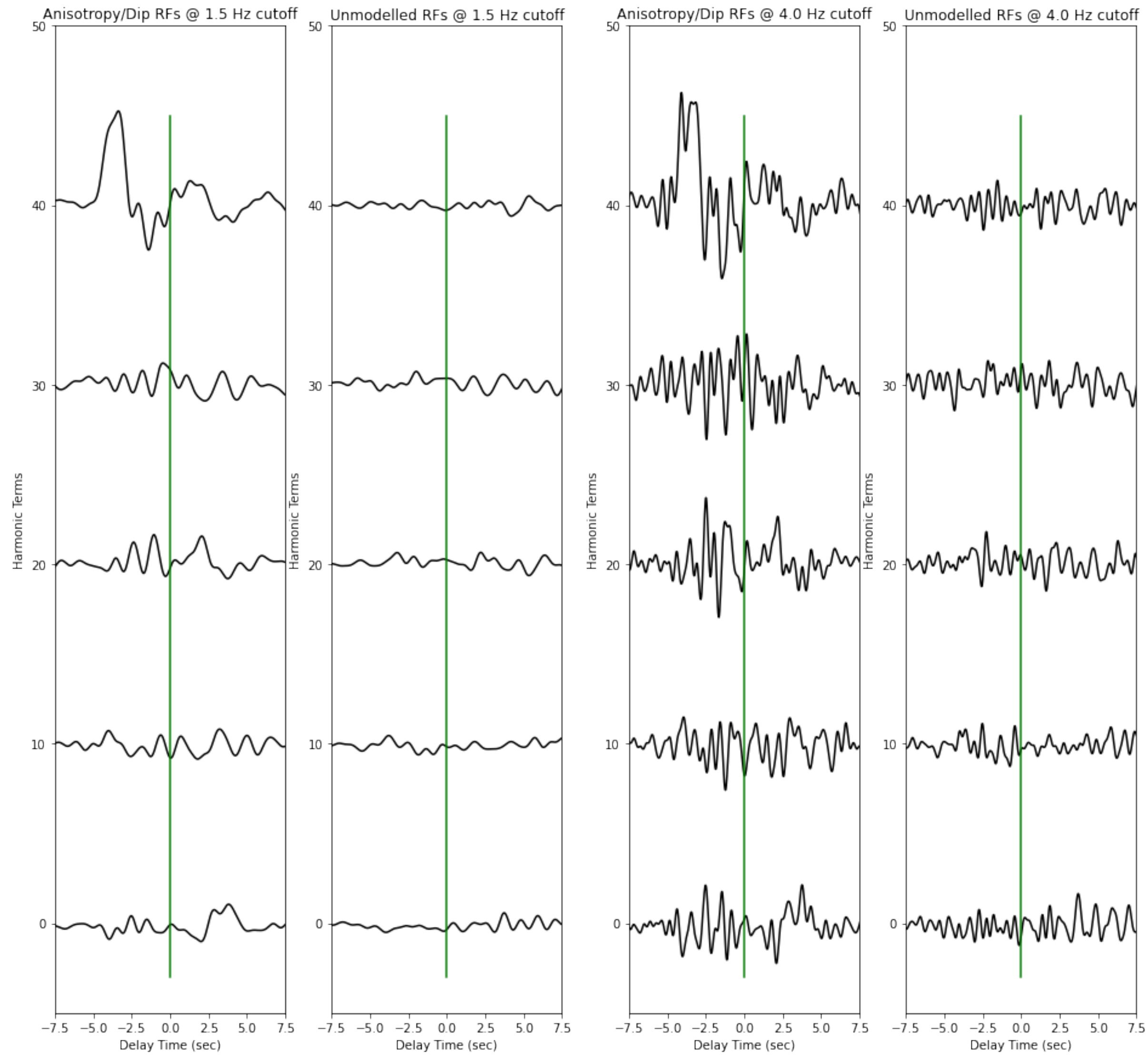


*Figure 15: Modelled and Unmodelled Receiver Functions for 1.5 and 4.0 Hz cutoffs for EGMT. There is tilted anisotropy of around 1 to 5%. There is horizontal anisotropy of about 1 to 3%. EGMT is very far away from the Yellowstone hotspot track in Northern Montana.*

cmin = -0.033240528111491634
cmax = 0.06993608351575675
2min = -0.01199823324546341
2max = 0.016070508800915408
2min = -0.010656455566407853
2max = 0.02193349132915427
4min = -0.011330648008332476
4max = 0.01087963388010979
4min = -0.013516279246506512
4max = 0.014129574056793222

cmin = -0.05448195400160206
cmax = 0.08362749506093199
2min = -0.040644277370395714
2max = 0.03767478791381298
2min = -0.0393924323157474
2max = 0.04938920073076056
4min = -0.03438693536924826
4max = 0.019810691669782336
4min = -0.029646377980345563
4max = 0.028511094091049346

*Elko, Nevada, USA (ELK)*

Start / End Date: 1994-01-06 / 2499-01-01

Elevation: 2210 m

Saved Events from 2014-2019: 608

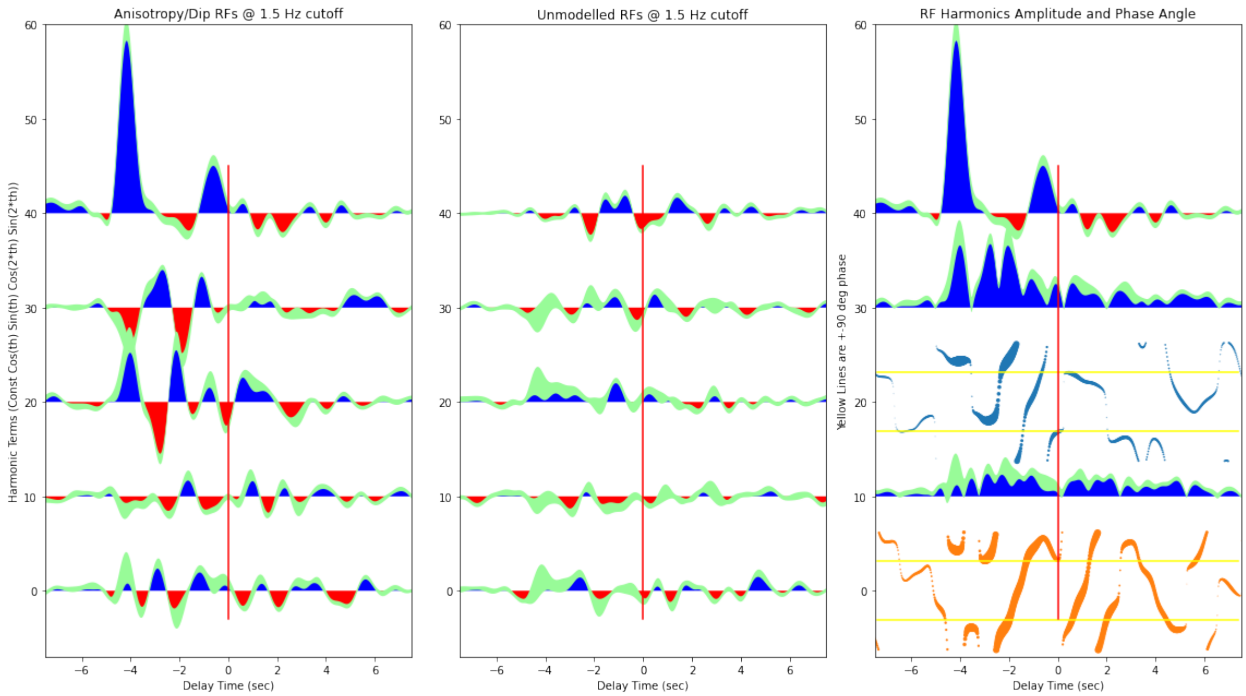


*Figure 16: Models of Anisotropy/Dip RFs, Unmodelled RFs, and RF Harmonics Amplitude and Phase Angle at 1.5 Hz cutoff Plots for ELK. The Moho appears to be around 35 km as indicated by the blue pulse at the 0 sec delay time. Further investigation is needed to explain the shift in the constant plots that model the isotropic structures between the modelled and unmodelled receiver functions. There is tilted anisotropy and horizontal anisotropy throughout the lower crust. Near the Moho, the anisotropic orientation within some of the layers are stable but not facing the same direction. There is some twisting near the Moho, but the twisting feature are broken up, suggesting that there are thinner layers with anisotropy.*

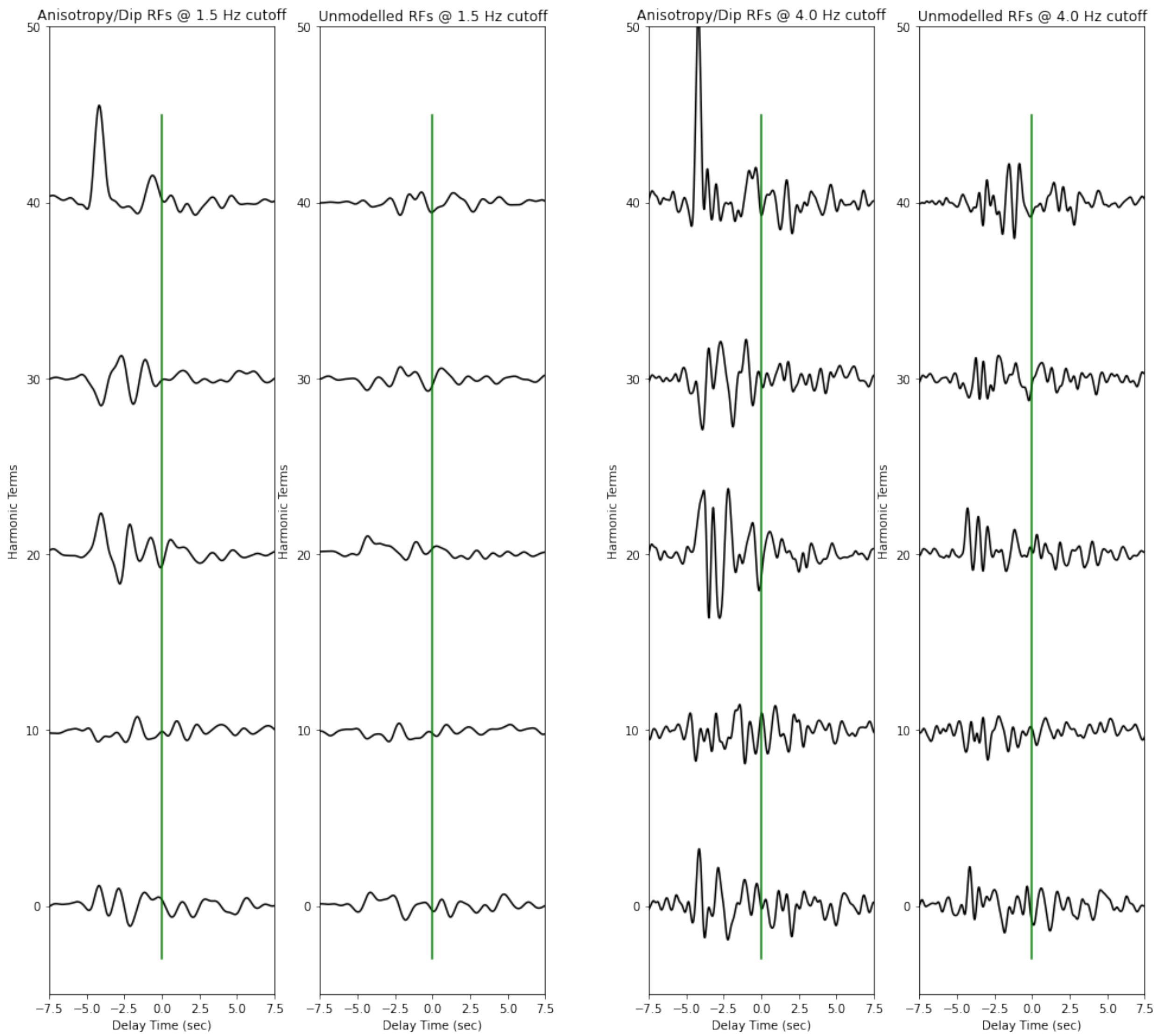


*Figure 17: Modelled and Unmodelled Receiver Functions for 1.5 and 4.0 Hz cutoffs for ELK. There is tilted anisotropy of around 2 to 5%. There is horizontal anisotropy of about 1 to 4%. ELK sits outside the hotspot track in northeastern Nevada, so anisotropic values are low.*

cmin = -0.009514530772746223
cmax = 0.07359751104270387
2min = -0.020684544787106456
2max = 0.017164130967546695
2min = -0.02243647438101042
2max = 0.031098919982916515
4min = -0.009200913351309185
4max = 0.010186991611029986
4min = -0.015268015232489905
4max = 0.015463429712629428

cmin = -0.023591577920214313
cmax = 0.14540989280982114
2min = -0.038905378337866246
2max = 0.0294047216866438
2min = -0.048428419210916826
2max = 0.04972249543254147
4min = -0.025414905991301934
4max = 0.019371436690130896
4min = -0.025643433147454486
4max = 0.0433285513816101

### *Hanford, Washington, USA (HAWA)*

Start / End Date: 1999-04-23 / 2499-01-01
Elevation: 364 m
Saved Events from 2014-2019: 601

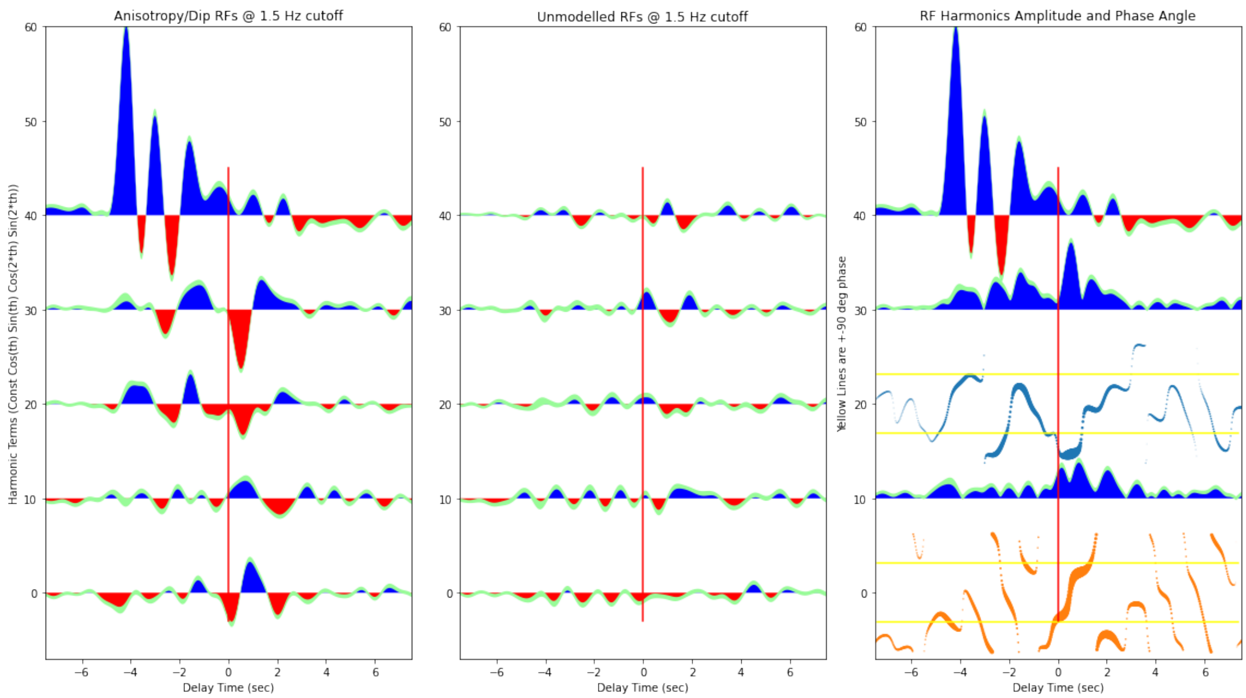


*Figure 18: Models of Anisotropy/Dip RFs, Unmodelled RFs, and RF Harmonics Amplitude and Phase Angle at 1.5 Hz cutoff Plots for HAWA. The Moho appears to be around 35 km as indicated by the blue pulse at the 0 sec delay time. There is tilted anisotropy and horizontal anisotropy throughout the crust. The anisotropic orientation within some of the layers are not stable and are not facing the same direction either.*

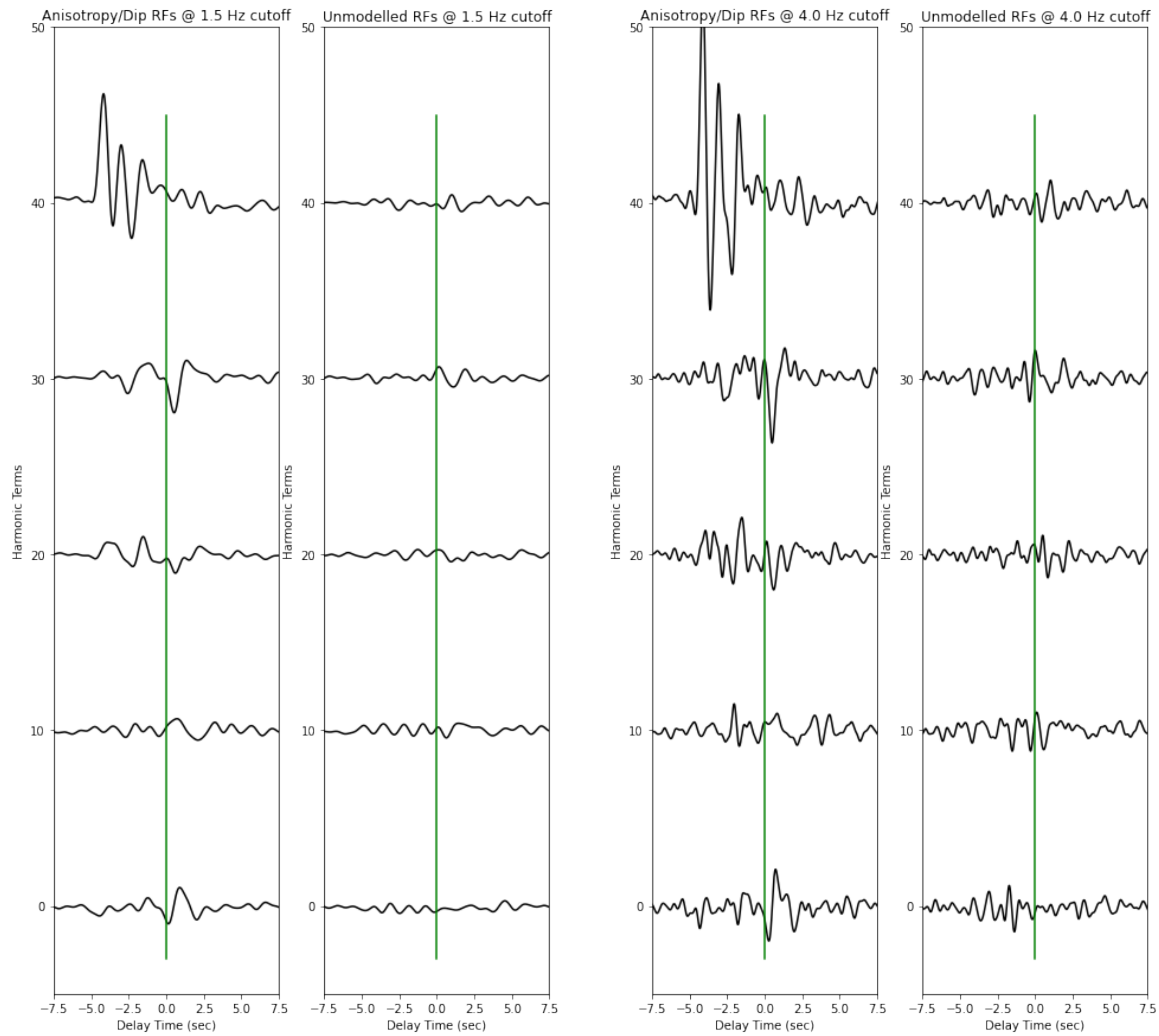


*Figure 19: Modelled and Unmodelled Receiver Functions for 1.5 and 4.0 Hz cutoffs for HAWA. There is tilted anisotropy of around 1 to 3% and horizontal anisotropy of around 1 to 2%. Anisotropic values are low given that HAWA is located in Washington State in the Columbia River Basalt Grou, where the crust is undisturbed.*

cmin = -0.026926639374118176
cmax = 0.08267132798294649
2min = -0.025836036639976596
2max = 0.013844145079046953
2min = -0.014183751078379523
2max = 0.013530559717428956
4min = -0.007472154664644538
4max = 0.008728625784582415
4min = -0.013428334977078002
4max = 0.014052018345536472

cmin = -0.08128693532808219
cmax = 0.162910554483092
2min = -0.0487682154712367
2max = 0.023177093813393276
2min = -0.026824056908857984
2max = 0.028106340716015036
4min = -0.012045021954637782
4max = 0.01999890398198686
4min = -0.02650980189185718
4max = 0.02789991732834158

*Hailey, Idaho, USA (HLID)*
Start / End Date: 1998-08-10 / 2499-01-01
Elevation: 1772 m
Saved Events from 2014-2019: 542

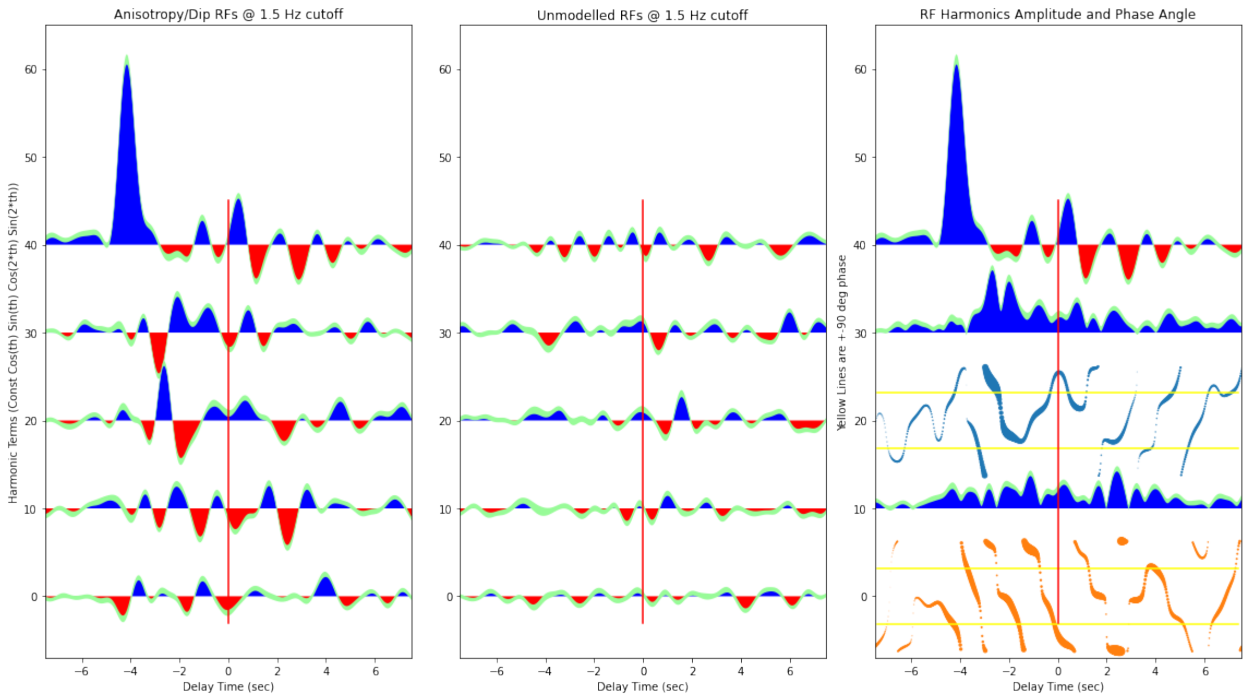


*Figure 20: Models of Anisotropy/Dip RFs, Unmodelled RFs, and RF Harmonics Amplitude and Phase Angle at 1.5 Hz cutoff Plots for HLID. The Moho appears to be around 35 km as indicated by the blue pulse at the 0 sec delay time. However, we are not certain that is where the Moho is, as it could be shallower. There is tilted anisotropy and horizontal anisotropy throughout the crust. There also appears to be anisotropy in the upper mantle. The anisotropic orientation within some of the layers are not stable and are not facing the same direction.*

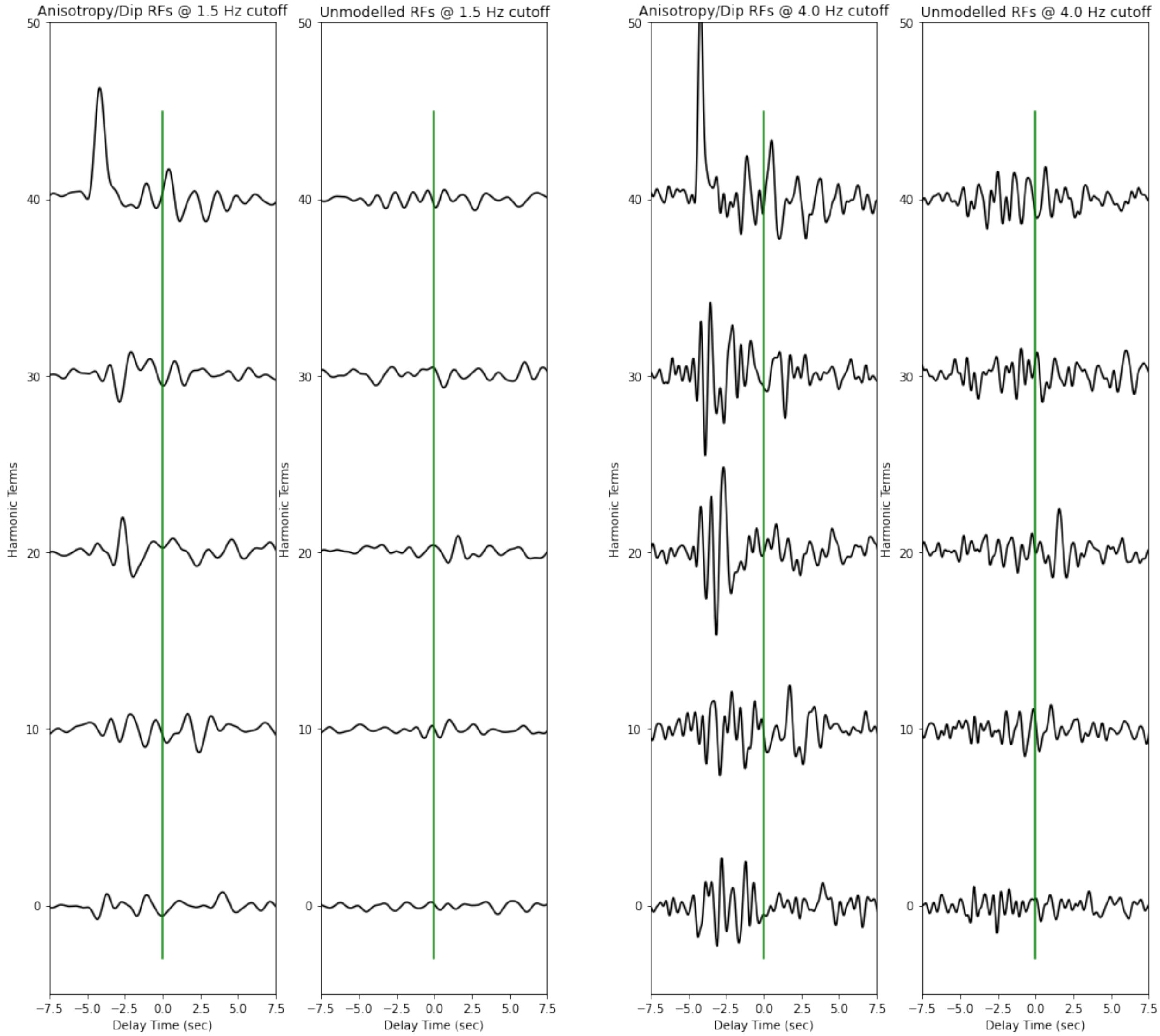


*Figure 21: Modelled and Unmodelled Receiver Functions for 1.5 and 4.0 Hz cutoffs for HLID. There is tilted anisotropy of around 1 to 3%. Horizontal anisotropy is around 1 to 4%. HLID is away from the Yellowstone uplift; it is found in central Idaho. However, it is close to an ancient caldera from around 6.5 million years ago, so anisotropic values are still modest.*

| | |
|---|---|
| cmin = -0.016910341772939423 | cmin = -0.030279199865110858 |
| cmax = 0.08412758042861192 | cmax = 0.15606728439701983 |
| 2min = -0.02002652407106427 | 2min = -0.06037025032255651 |
| 2max = 0.01777163676043065 | 2max = 0.05525370854896747 |
| 2min = -0.01869382065201058 | 2min = -0.06247503610550624 |
| 2max = 0.026321564958816927 | 2max = 0.06431090324787328 |
| 4min = -0.017882609826022033 | 4min = -0.03534313950705223 |
| 4max = 0.01148689989010758 | 4max = 0.032983818125313084 |
| 4min = -0.010469711593056798 | 4min = -0.030489744994492522 |
| 4max = 0.010066969972493454 | 4max = 0.0355795384877211 |

*Hardware Ranch, Cache County, Utah, USA (HWUT)*

Start / End Date: 1997-03-26 / 2499-01-01

Elevation: 1830 m

Saved Events from 2014-2019: 589

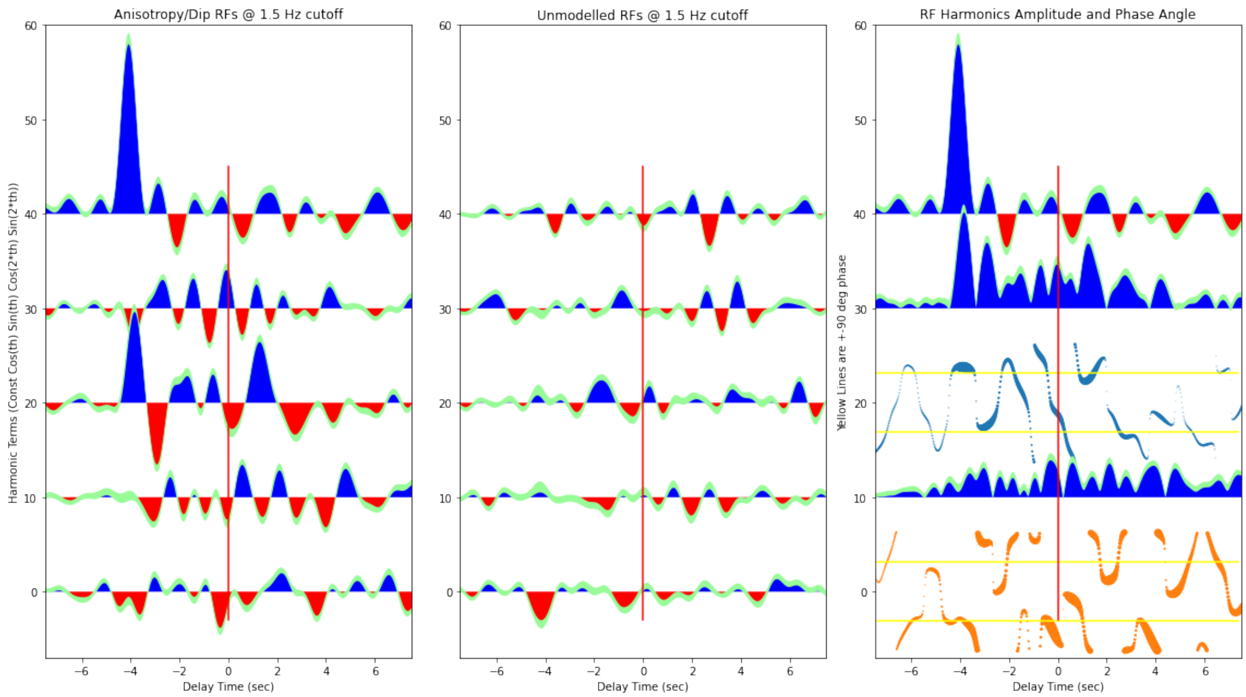


*Figure 22: Models of Anisotropy/Dip RFs, Unmodelled RFs, and RF Harmonics Amplitude and Phase Angle at 1.5 Hz cutoff Plots for HWUT. The Moho appears to be around 35 km as indicated by the blue pulse at the 0 sec delay time. There is significant tilted anisotropy and horizontal anisotropy throughout the lower crust. In the mantle, there is also anisotropy, both tilted and horizontal. The anisotropic orientation within some of the layers are not stable and are not facing the same direction.*

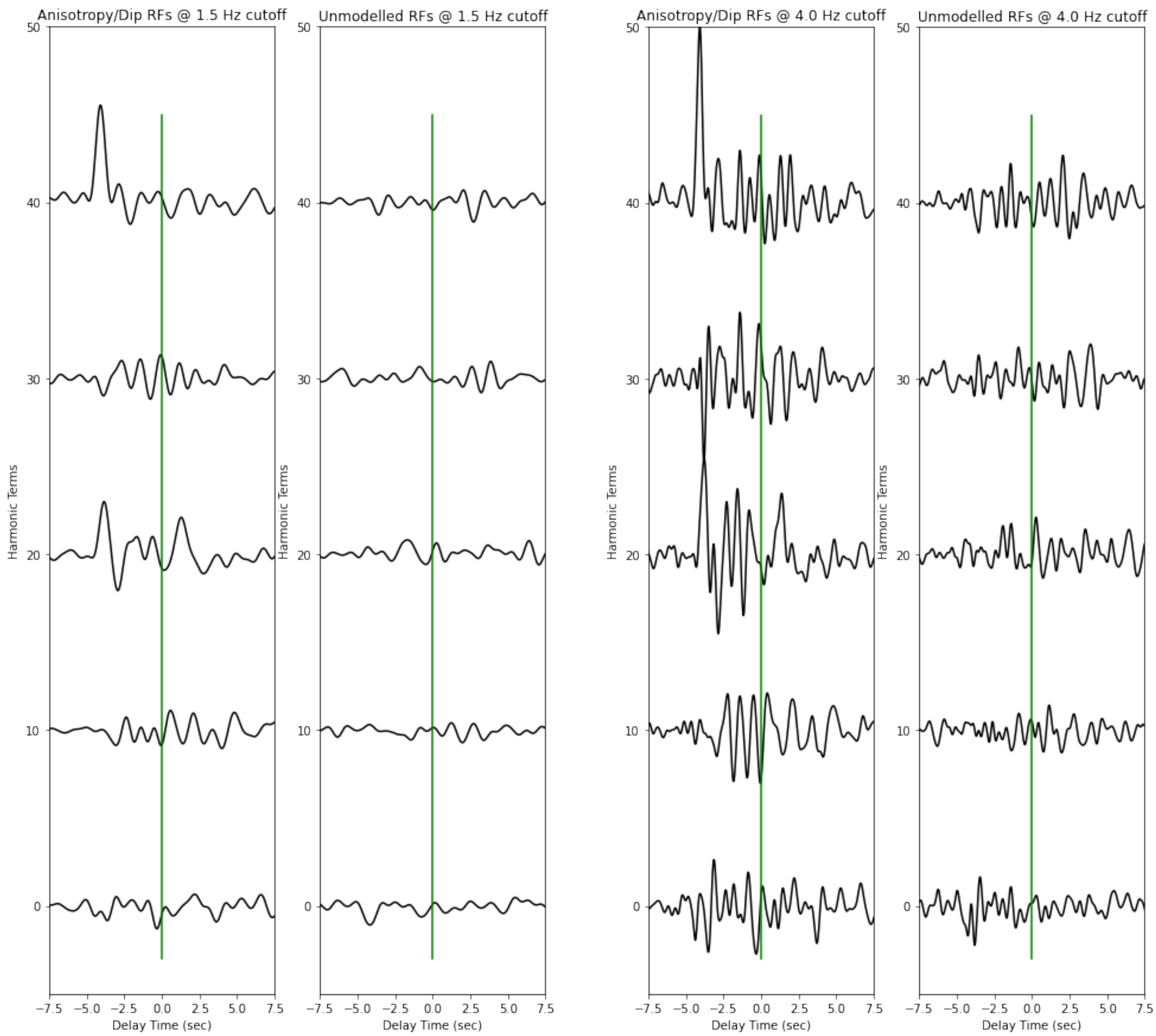


*Figure 23: Modelled and Unmodelled Receiver Functions for 1.5 and 4.0 Hz cutoffs for HWUT. There is tilted anisotropy around 2 to 7% and horizontal anisotropy of 1 to 4%. HWUT is near the hotspot track, which helps to explain the relatively higher anisotropic values.*

cmin = -0.01649635958684242
cmax = 0.07375678291952215
2min = -0.01578239314438582
2max = 0.017841493015046964
2min = -0.02754837339712641
2max = 0.03985634219787599
4min = -0.013878082448083726
4max = 0.014928531574891109
4min = -0.01726247462951534
4max = 0.008949335503749867

cmin = -0.030987221489499256
cmax = 0.1344818389269331
2min = -0.0633268740328584
2max = 0.05028473182559776
2min = -0.060142293261389417
2max = 0.07266631373128646
4min = -0.04026747698617464
4max = 0.028201181705842487
4min = -0.0363846608676785
4max = 0.035118860203809533

*LASA Array, Montana, USA (LAO)*
Start / End Date: 2004-07-15 / 2499-01-01
Elevation: 902 m
Saved Events from 2014-2019: 587

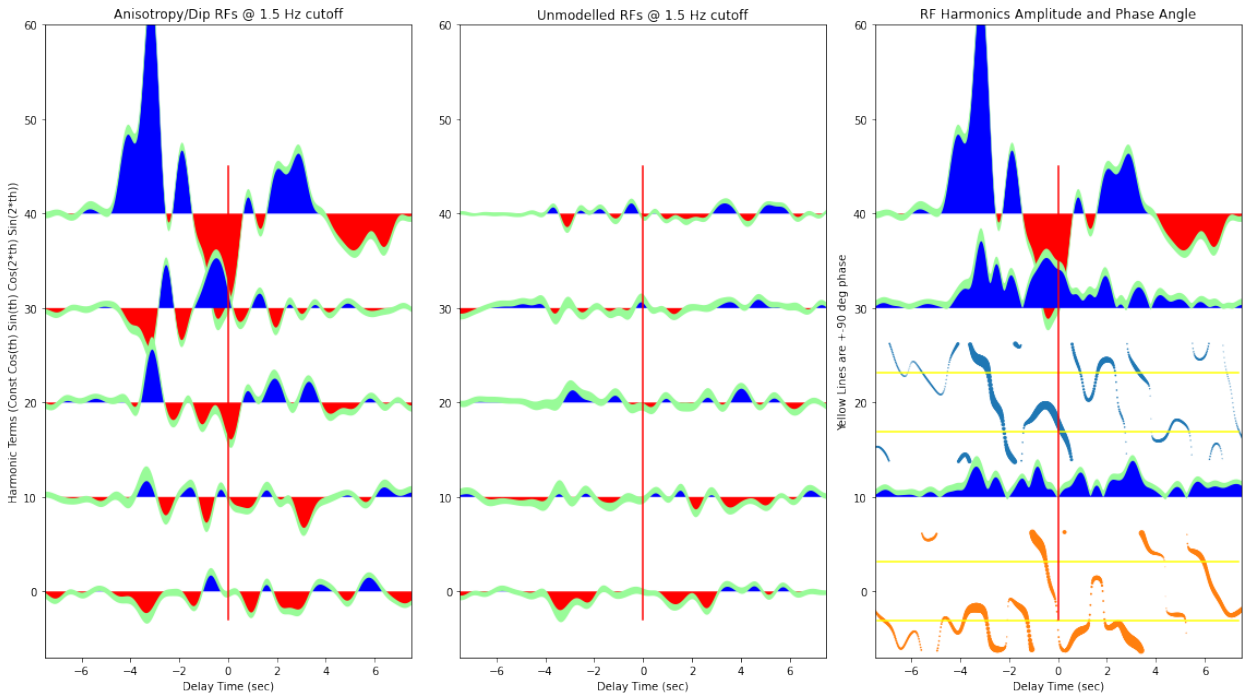


*Figure 24: Models of Anisotropy/Dip RFs, Unmodelled RFs, and RF Harmonics Amplitude and Phase Angle at 1.5 Hz cutoff Plots for LAO. At the target depth of 35 km as indicated by the blue pulse at the 0 sec delay time, there is a large red pulse, suggesting that this is a low-velocity zone. This means the Moho might be deeper than 35km at around 2 to 4 seconds. There is tilted anisotropy and horizontal anisotropy throughout the lower crust. There is a large red pulse under the Moho, suggesting there may be a hot mantle as denoted by the low velocities. The anisotropic orientation within some of the layers are stable near the target depth but not facing the same direction.*

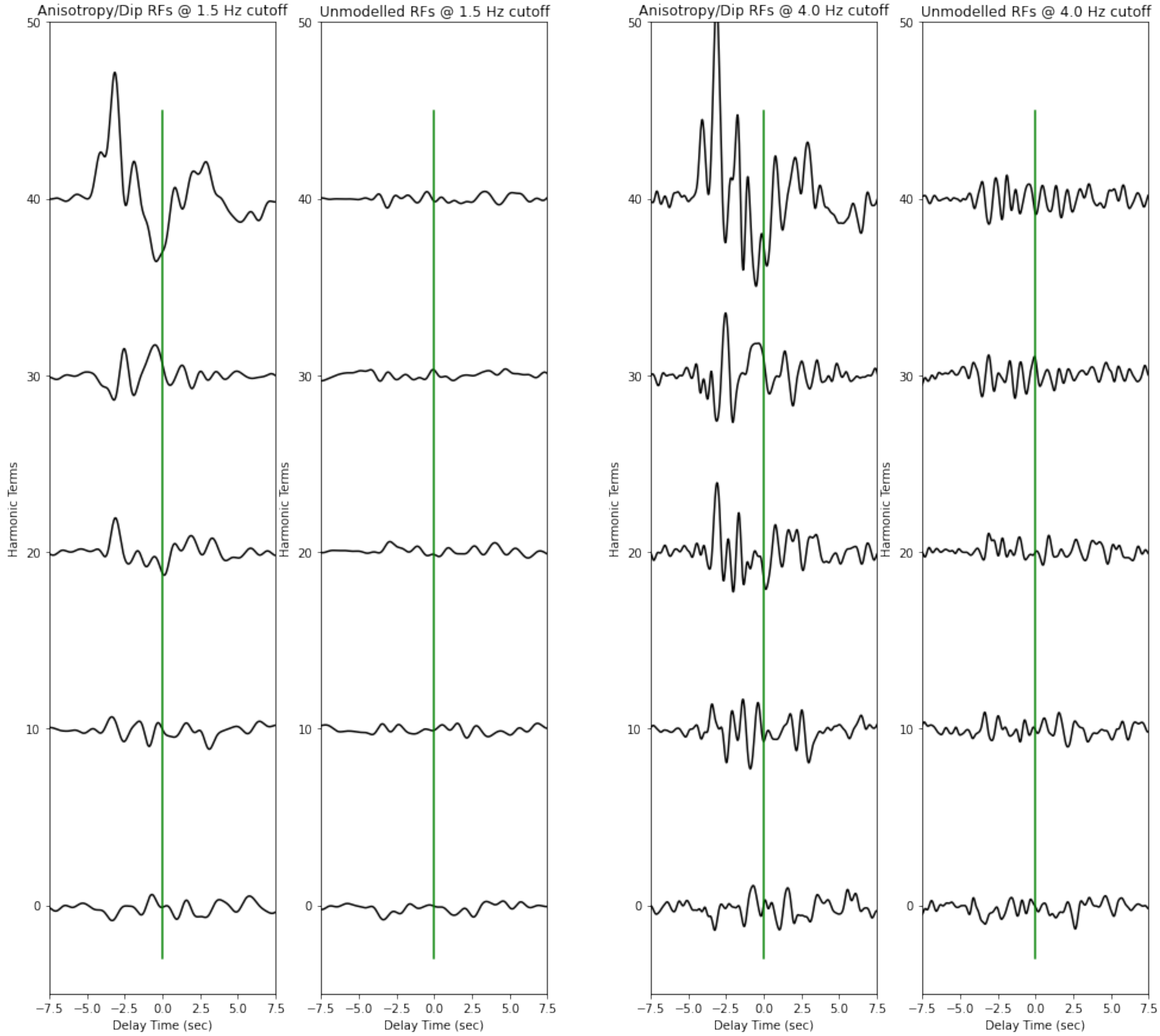


*Figure 25: Modelled and Unmodelled Receiver Functions for 1.5 and 4.0 Hz cutoffs for LAO. Tilted anisotropy is around 2 to 5% and horizontal anisotropy of 1 to 2%. LAO is located in the future pathway of the hotspot track, meaning there is a good chance in the next couple of millions of years, there will be a new caldera near or on top of LAO. However, for now, anisotropic values are low.*

| | |
|---|---|
| cmin = -0.04734514484090763 | cmin = -0.06602649580715723 |
| cmax = 0.09532086920624339 | cmax = 0.15123213814910272 |
| 2min = -0.018579508672327404 | 2min = -0.035481085250219216 |
| 2max = 0.022994658482030673 | 2max = 0.04705670743711676 |
| 2min = -0.017439108911468416 | 2min = -0.030033665597405192 |
| 2max = 0.025738066043694358 | 2max = 0.052257343888304324 |
| 4min = -0.015446429455397672 | 4min = -0.030217722711956677 |
| 4max = 0.008975679475310791 | 4max = 0.0222611786005357 |
| 4min = -0.011449056738993676 | 4min = -0.018716473030989077 |
| 4max = 0.008243653850388407 | 4max = 0.01497963064753143 |

*Lake (Yellowstone—Lake), Yellowstone National Park, Wyoming (LKWY)*

Start / End Date: 1995-10-11 / 2499-01-01

Elevation: 2424 m

Saved Events from 2014-2019: 507

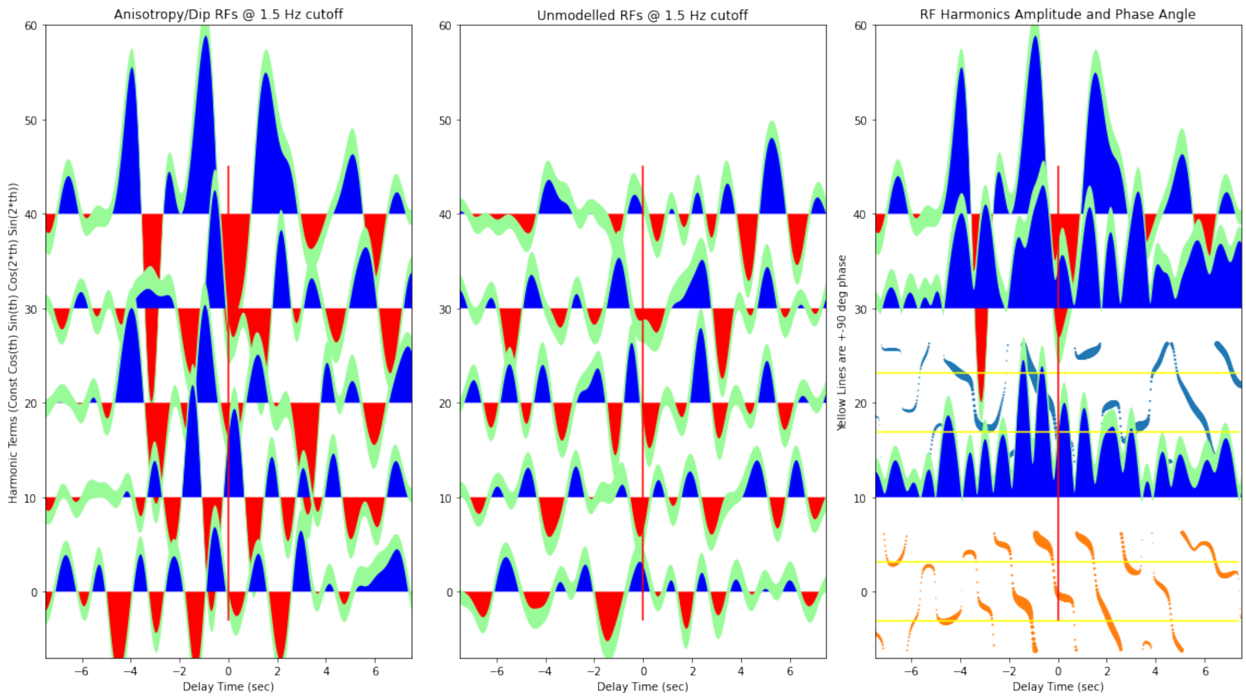


*Figure 26: Models of Anisotropy/Dip RFs, Unmodelled RFs, and RF Harmonics Amplitude and Phase Angle at 1.5 Hz cutoff Plots for LKWY. It is unclear where the Moho is as there is a large red pulse at the target depth, meaning this is a low-velocity zone. Perhaps the Moho is lower than 35km, but it could also be slightly shallower. There is tilted anisotropy and horizontal anisotropy throughout the lower crust. Note that LKWY is located in the Yellowstone caldera, so the waveforms are rather unusual. The waveforms for LKWY were abnormal because it sits within the caldera, so there might be additional considerations around the ground motion. This is reinforced by the large amplitudes shown on the plots for the absolute values for the two-lobed and four-lobed amplitudes. The anisotropic orientation within some of the layers are not stable and are not facing the same direction.*

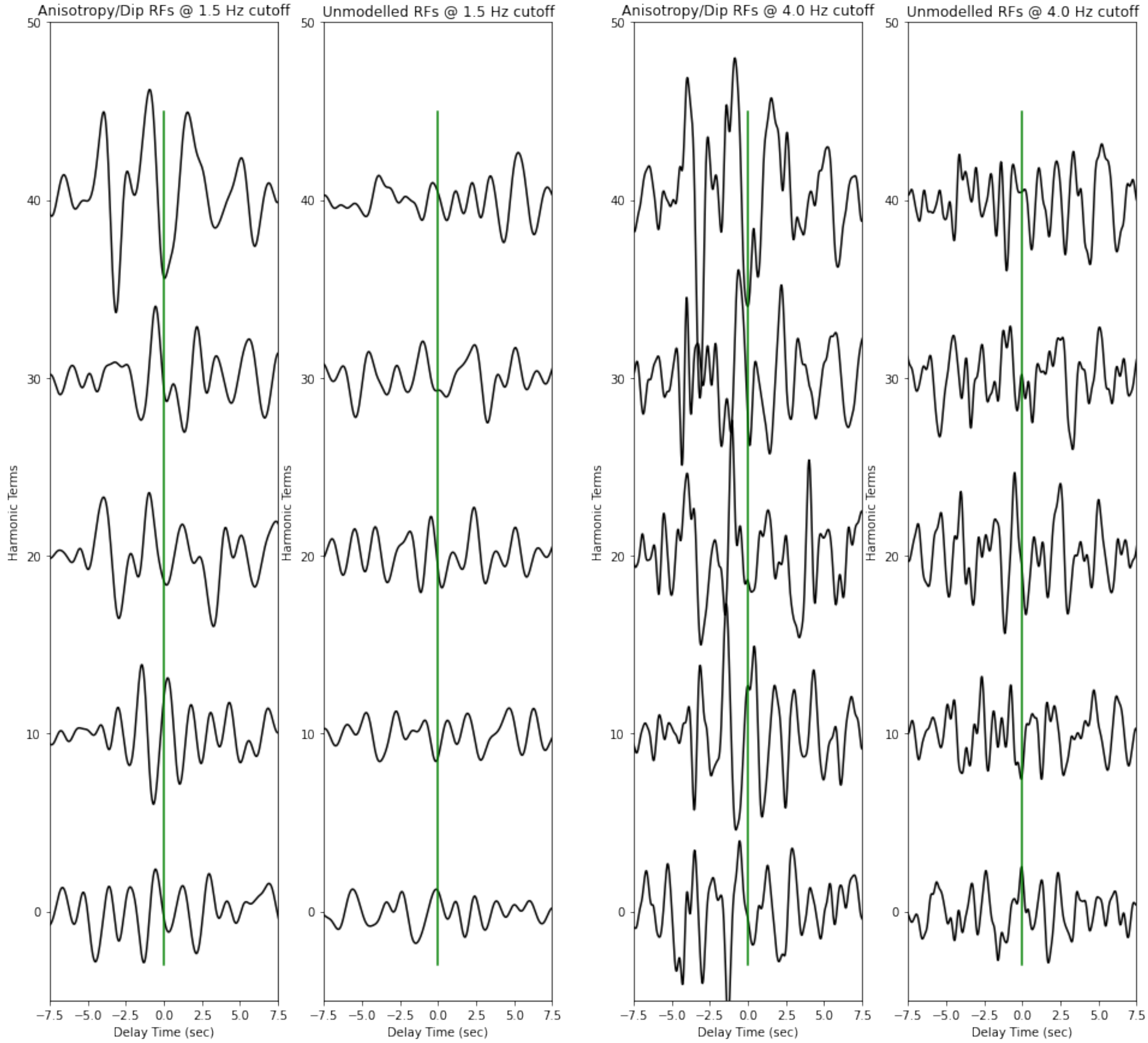


*Figure 27: Modelled and Unmodelled Receiver Functions for 1.5 and 4.0 Hz cutoffs for LKWY. Tilted and horizontal anisotropy values are both around 5-10%, which suggest significant anisotropic layering. This makes sense because LKWY sits directly on top of the caldera on the hotspot track.*

cmin = -0.08435805728087847
cmax = 0.08282270683843407
2min = -0.04063800308337281
2max = 0.05367953540708041
2min = -0.05295978448086632
2max = 0.04728385089337349
4min = -0.052867027176391995
4max = 0.05170199786589817
4min = -0.038273863490347726
4max = 0.031773416585692

cmin = -0.14835443666167733
cmax = 0.10644989447890052
2min = -0.06539549717587238
2max = 0.08098108551390612
2min = -0.06677799761073291
2max = 0.10164577936412404
4min = -0.07208755663018468
4max = 0.09741408055098398
4min = -0.08018406579912193
4max = 0.05294610034174238

*Missoula, Montana, USA (MSO)*
Start / End Date: 2002-08-23 / 2002-08-23
Start / End Date: 2002-08-23 / 2499-01-01
Elevation: 1264 m
Saved Events from 2014-2019: 605

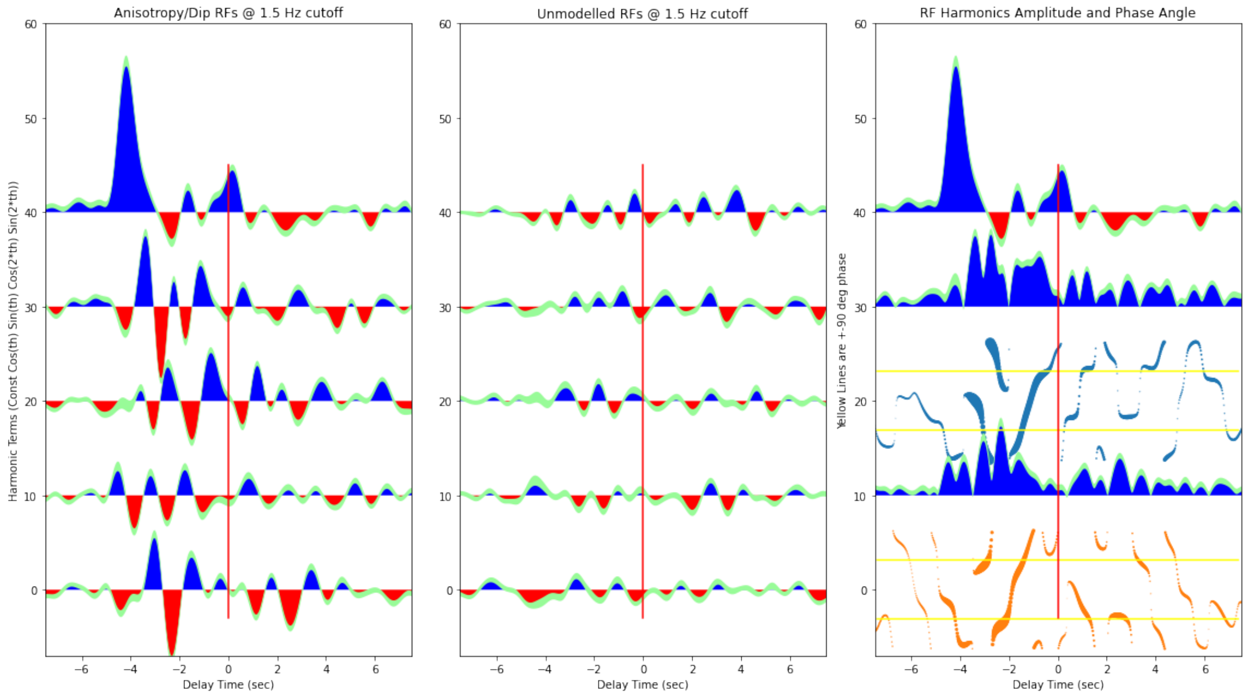


*Figure 28: Models of Anisotropy/Dip RFs, Unmodelled RFs, and RF Harmonics Amplitude and Phase Angle at 1.5 Hz cutoff Plots for MSO. The Moho appears to be around 35 km as indicated by the blue pulse at the 0 sec delay time. There is tilted anisotropy and horizontal anisotropy throughout the lower crust. The anisotropic orientation within some of the layers are not stable and are not facing the same direction.*

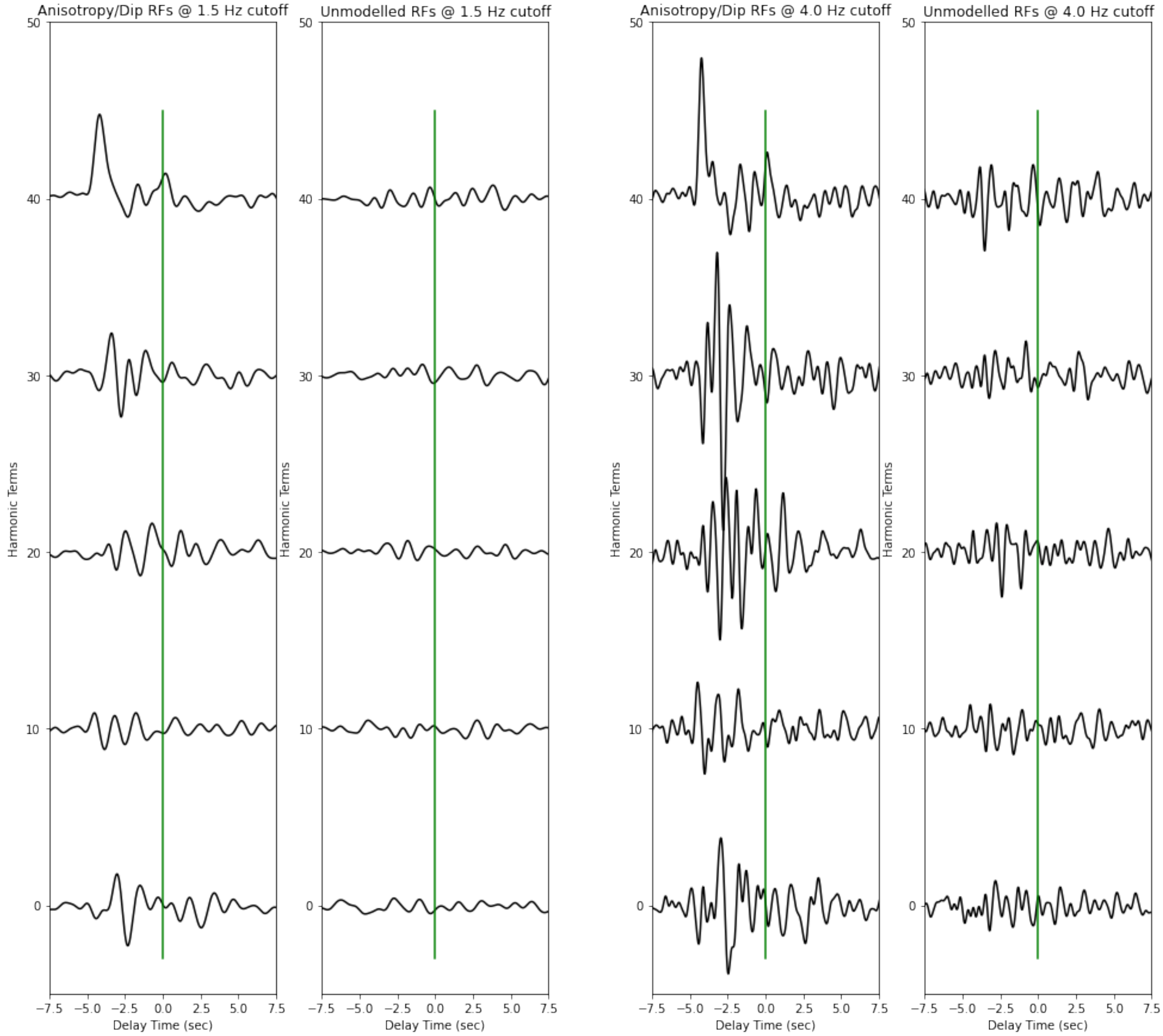


*Figure 29: Modelled and Unmodelled Receiver Functions for 1.5 and 4.0 Hz cutoffs for MSO. Tilted anisotropy is around 2-9% and horizontal anisotropy is around 1-5%. Despite not being on the Yellowstone hotspot, MSO has relatively high tilted anisotropy. Further investigation is needed to understand why this is the case.*

cmin = -0.013789976316839528
cmax = 0.06361091105921729
2min = -0.03138478195951358
2max = 0.03187266412540471
2min = -0.017797307556172287
2max = 0.021662328768482942
4min = -0.015626656040027883
4max = 0.011957007788989183
4min = -0.030421709471212335
4max = 0.0237439189623192

cmin = -0.027107085498816186
cmax = 0.10619497918641994
2min = -0.11698557596249184
2max = 0.09272694605612719
2min = -0.06626327298384962
2max = 0.05623636100847836
4min = -0.034142134654020266
4max = 0.0350649629932596
4min = -0.05159631574554653
4max = 0.05092014512603186

*Newport, Washington, USA (NEW)*
Start / End Date: 1993-11-13 / 2499-01-01
Elevation: 760 m
Saved Events from 2014-2019: 604

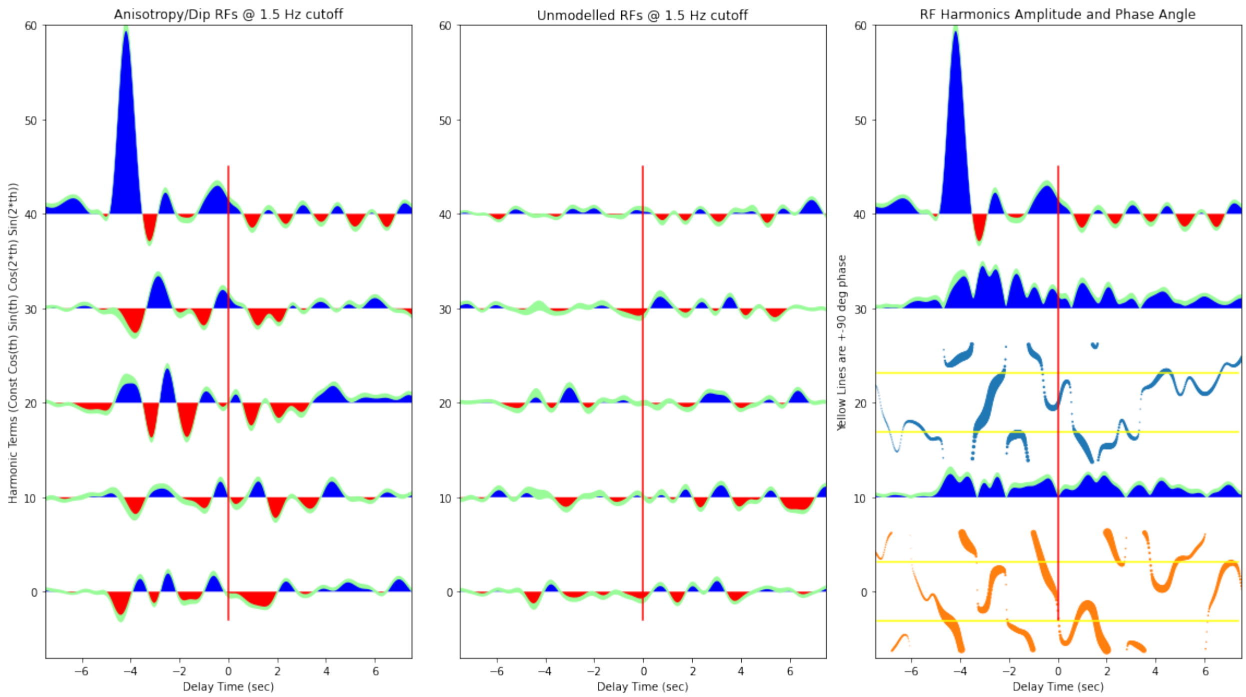


*Figure 30: Models of Anisotropy/Dip RFs, Unmodelled RFs, and RF Harmonics Amplitude and Phase Angle at 1.5 Hz cutoff Plots for NEW. The Moho appears to be around 35 km as indicated by the blue pulse at the 0 sec delay time. There is tilted anisotropy and horizontal anisotropy throughout the lower crust. The anisotropic orientation within some of the layers are not stable and not facing the same direction.*

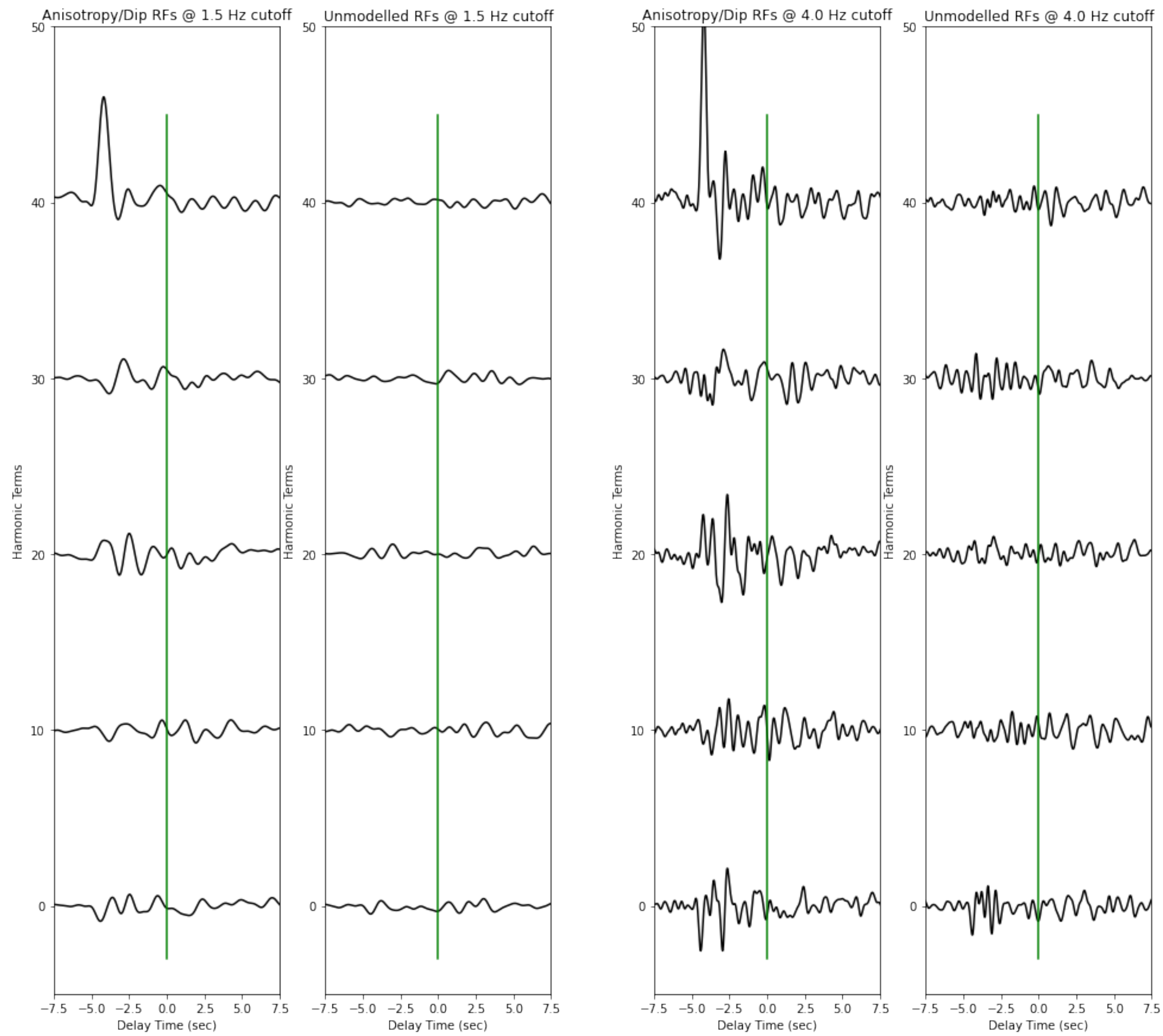


*Figure 31: Modelled and Unmodelled Receiver Functions for 1.5 and 4.0 Hz cutoffs for NEW. Tilted anisotropy is around 1-5%, and horizontal anisotropy is around 1-2%. Anisotropic values are low because NEW is located very far from the hotspot track, in the northeastern region of Washington State.*

cmin = -0.012888286075906131
cmax = 0.07998346688689606
2min = -0.011585115778660745
2max = 0.014673210558164547
2min = -0.015826145118169786
2max = 0.015759458701511863
4min = -0.009676790262760547
4max = 0.007698795421359571
4min = -0.011581656410293737
4max = 0.008780116018856369

cmin = -0.04289156944978323
cmax = 0.15447921073344895
2min = -0.020186671046168437
2max = 0.022041992851557 26
2min = -0.03649319961817289
2max = 0.045230206811922594
4min = -0.022918495525867152
4max = 0.023671119741100324
4min = -0.0339986354253804
4max = 0.028464440571540843

*Red Lodge, Montana, USA (RLMT)*
Start / End Date: 2006-09-12 / 2499-01-01
Start / End Date: 2006-09-12 / 2999-12-31
Start / End Date: 2006-08-24 / 2599-12-31
Elevation: 2086 m
Saved Events from 2014-2019: 597

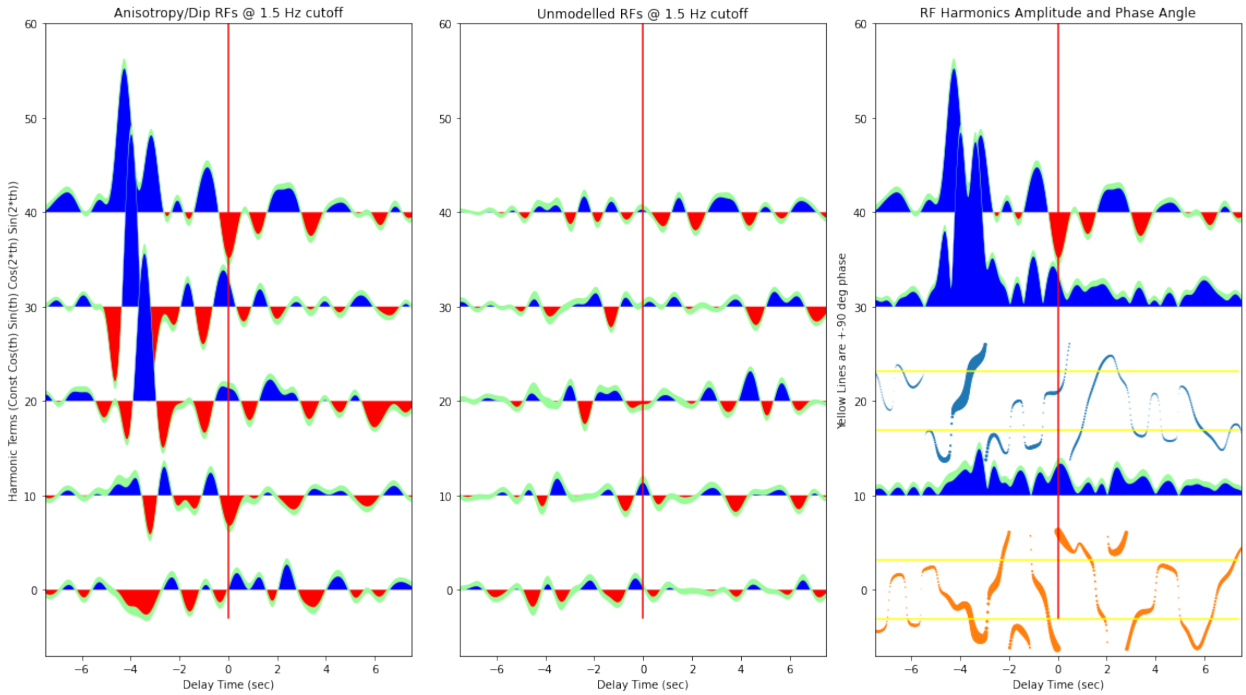


*Figure 32: Models of Anisotropy/Dip RFs, Unmodelled RFs, and RF Harmonics Amplitude and Phase Angle at 1.5 Hz cutoff Plots for RLMT. The Moho may be deeper than 35km as indicated by the blue pulse at around 2-3 seconds. At 0 seconds, there is a low-velocity zone. There are large signals in the top 10km of the crust. There is strong anisotropic layering at shallow crustal depths, less than 15km beneath RLMT. The anisotropic orientation within some of the layers are not stable and not facing the same direction.*

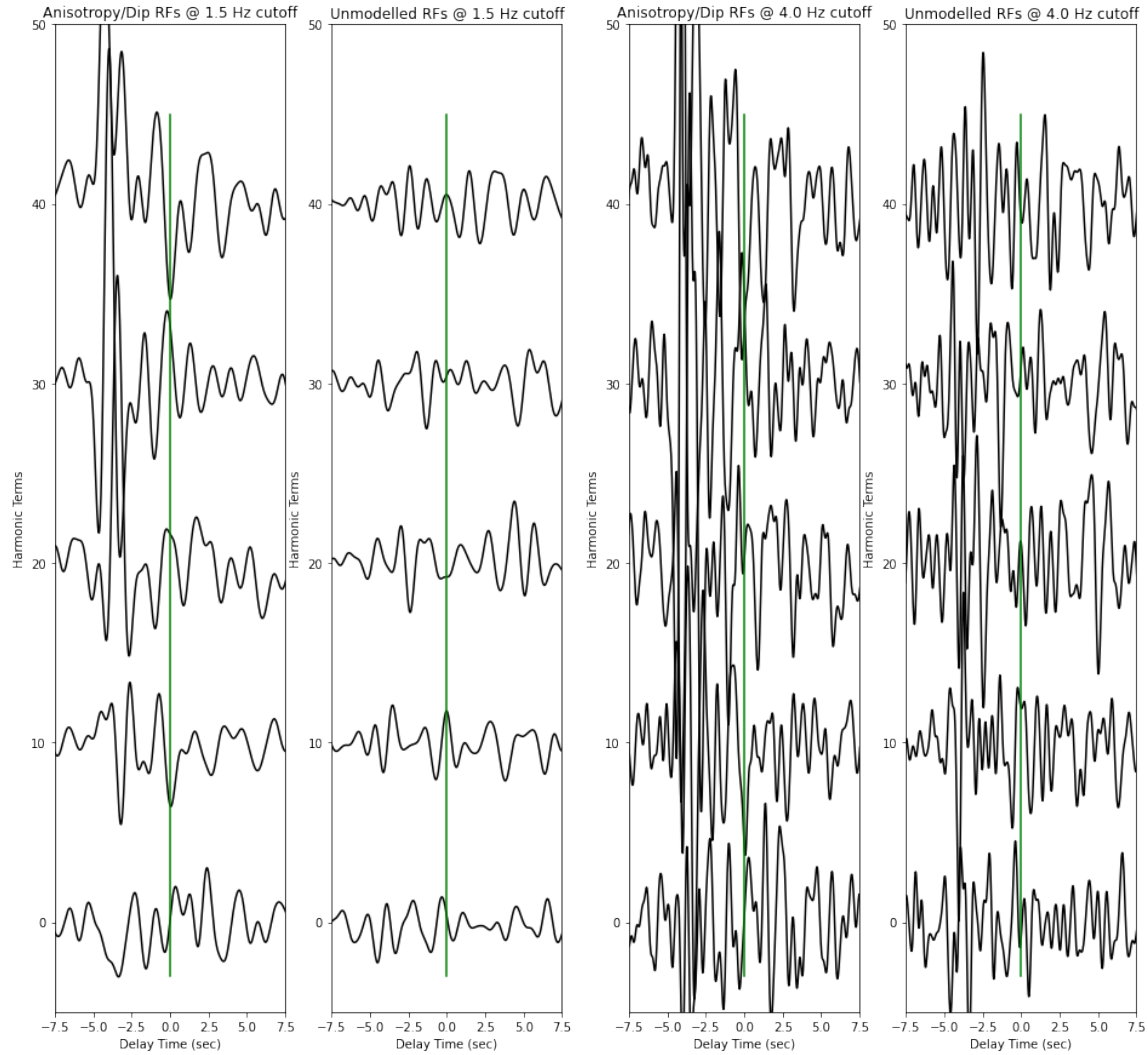


*Figure 33: Modelled and Unmodelled Receiver Functions for 1.5 and 4.0 Hz cutoffs for RLMT. Both frequency cutoffs show the same features of extremely high anisotropy in the lower crust especially for the two-lobe. The greater frequency cutoff plot has higher unmodelled energy, a much lower signal to noise ratio. Tilted anisotropy is 6-21% and horizontal anisotropy is 1-4%. RLMT has significant anisotropic layering, which makes sense since it sits on the uplift.*

cmin = -0.021199410720380656
cmax = 0.06291993537896504
2min = -0.03863100690987941
2max = 0.07456854190466931
2min = -0.020694560137347096
2max = 0.06404194417604887
4min = -0.018211335233019064
4max = 0.013440108017738692
4min = -0.012154083971470145
4max = 0.012110176296673039

cmin = -0.03469509378901751
cmax = 0.13585939029373797
2min = -0.08349749195473412
2max = 0.21193077848970482
2min = -0.05534971554003999
2max = 0.10469694462609655
4min = -0.05712457529311587
4max = 0.03931281685203486
4min = -0.03218667891977048
4max = 0.026473866276246576

*Wild Horse Valley, Oregon, USA (WVOR)*
Start / End Date: 1994-06-22 / 2499-01-01
Elevation: 1344 m
Saved Events from 2014-2019: 588

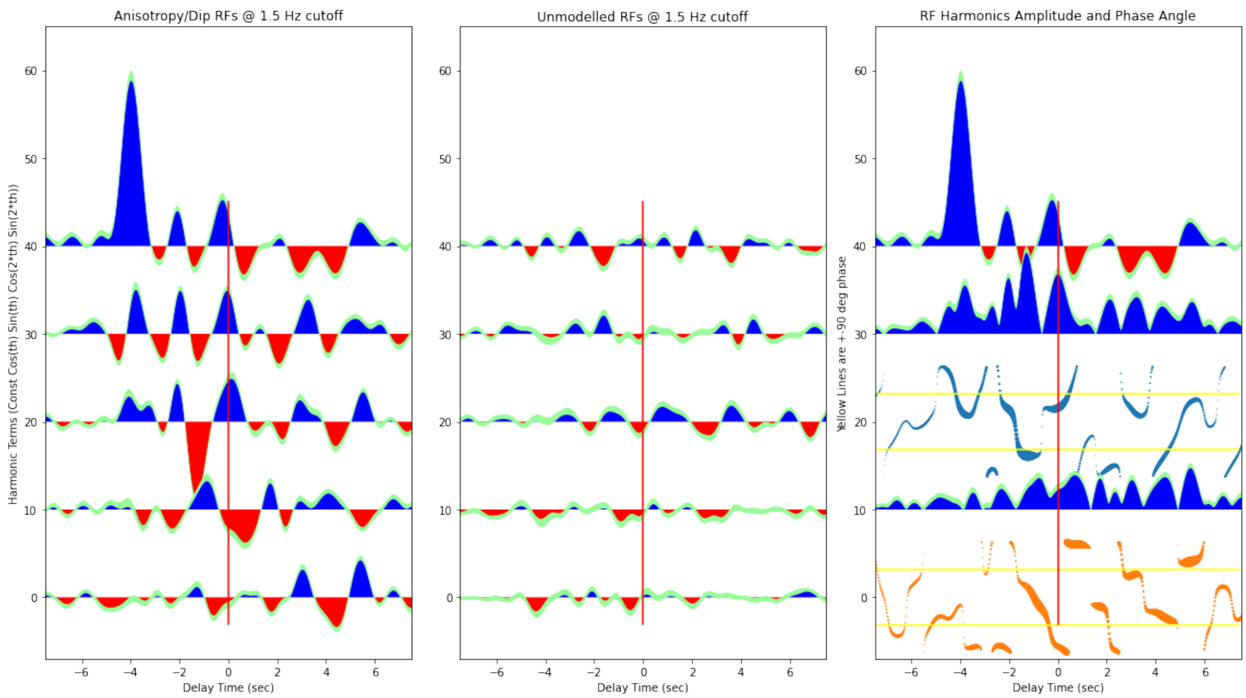


*Figure 34: Models of Anisotropy/Dip RFs, Unmodelled RFs, and RF Harmonics Amplitude and Phase Angle at 1.5 Hz cutoff Plots for WVOR. The Moho appears to be around 35 km as indicated by the blue pulse at the 0 sec delay time. There is tilted anisotropy and horizontal anisotropy throughout the lower crust. The anisotropic orientation within some of the layers are not stable and not facing the same direction.*

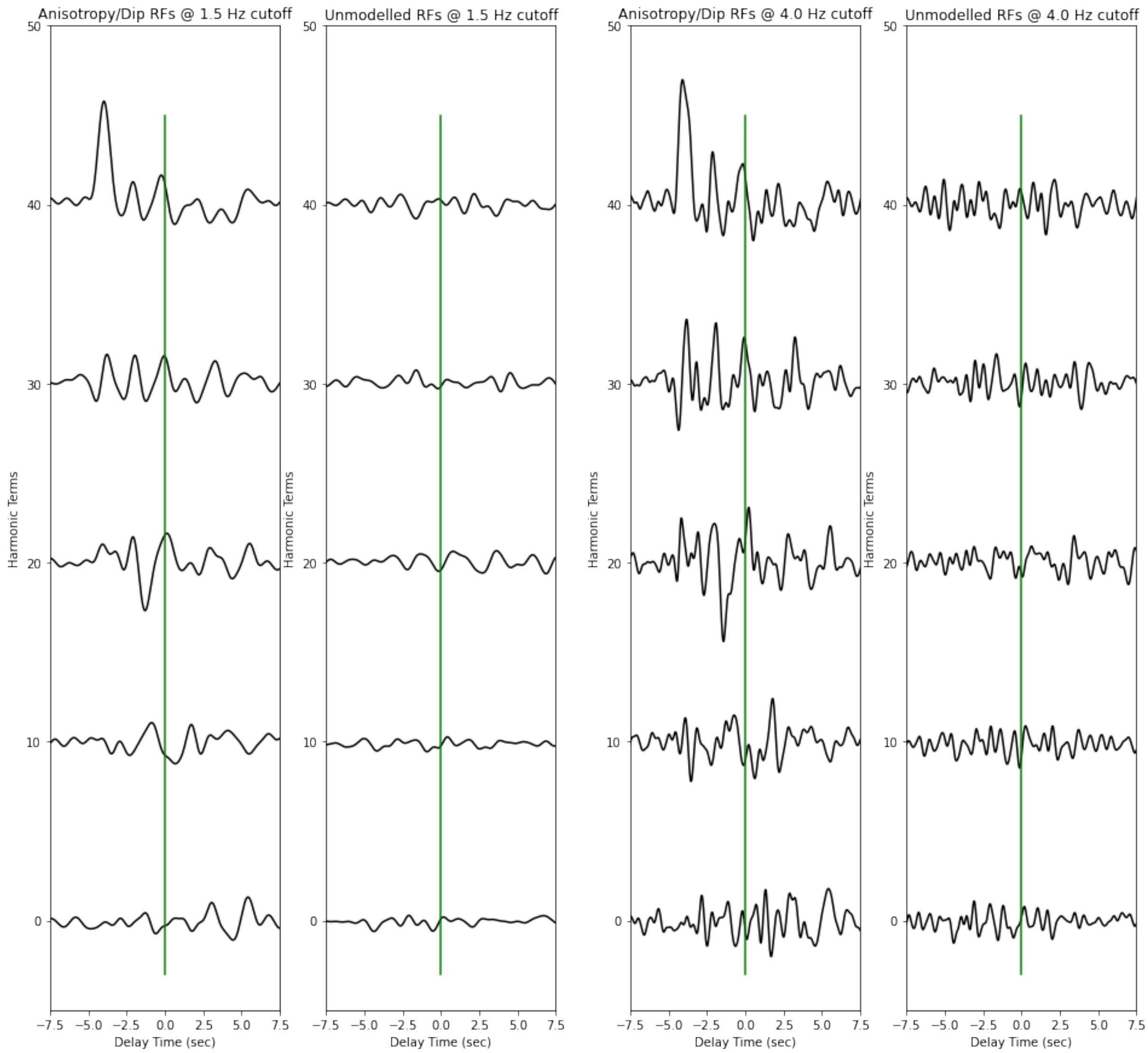


*Figure 35: Modelled and Unmodelled Receiver Functions for 1.5 and 4.0 Hz cutoffs for WVOR. Tilted anisotropy is 2-5% and horizontal anisotropy is 1-3%. WVOR is located on stable and undisturbed crust in the Columbia River basalt field, so anisotropic values are low.*

cmin = -0.014642340566232901
cmax = 0.07701100088932974
2min = -0.01421043275529406
2max = 0.02178694874565353
2min = -0.0357207827982309
2max = 0.021852062060197526
4min = -0.016381863981722325
4max = 0.014161377061136569
4min = -0.014425022889587781
4max = 0.017541337161379598

cmin = -0.02688237691757959
cmax = 0.09302717445809469
2min = -0.034672377931847916
2max = 0.04795328372632421
2min = -0.058700477946582404
2max = 0.04120056429775786
4min = -0.029576577813001742
4max = 0.03214210962655262
4min = -0.026670428792542108
4max = 0.023821024024359348

## Conclusion

Overall, the amplitudes of the "unmodelled" combination of radial and transverse receiver functions compared the "modelled" receiver functions are small. This supports our theory that there is anisotropy in the region. However, several stations in the Pacific Northwest had low two-lobed and four-lobed Ps amplitude variations which modelled the tilted and horizontal anisotropies, respectively. These stations including HAWA, WVOR, and BMO were located on stable and undisturbed crust, specifically in the Columbia River Basalt Group. RLMT had the highest anisotropic values. Strong two-lobed Ps amplitude variation at RLMT is consistent with tilted-axis anisotropy up 21%. AHID also had strong two-lobed Ps amplitude variation with tilted anisotropy up 10%. These two stations sit along the hotspot track, both bookending the caldera where LKWY sits. Some stations including AHID had a low-velocity zone slightly above the Moho. This hypothesis is not completely unfounded as Maguire et al. (2022) concluded that a low-velocity zone can be inferred above the Moho that has partial basaltic melt near the caldera. AHID is located around the site of the partial melt area.

Further research needs to be completed regarding the location of the Moho for some of the stations, including EGMT, HLID, LAO, and RLMT. For these stations, the Moho could be shallower or deeper than 35km. Additionally, there are interesting signals in the mantle, so future research should review the modelled receiver functions at depths greater than 35km.

## Acknowledgements

Words cannot fully describe the immense privilege it was to have been surrounded by the deeply caring and supportive people of the Earth and Planetary Sciences Department at Yale. While I did not come into college knowing I would pursue a degree in earth sciences, I quickly found a footing in the door through Professors Maureen Long and David Bercovici. I am thankful to Sophie Westacott and Elvira Mulyukova for guiding me on my first geology field trip, allowing me to foster a deeper connection with the academics right before the world shut down.

And when the world did shut down, I am incredibly thankful for Professor Jeffrey Park and Will Frazer for getting me through unprecedented times. To Professor Park, I cannot thank you enough for helping me develop my intellectual curiosity. Thank you for the unwavering support in shaping me to be a better researcher and person, one who approaches all questions equally without discrimination.

Once again, thank you Professor Long for bookending my Yale career as my second reader. Additionally, I want to thank the Karen Von Damm Fellowship and Professor Pincelli Hull for supporting this thesis at the American Geophysical Union Fall 2022 conference, where I delivered an oral presentation.

## References

Bannister, Stephen, Edward A. Bertrand, Sebastian Heimann, Sandra Bourguignon, Cameron Asher, Jackson Shanks, and Adrian Harvison. 2022. “Imaging Sub-Caldera Structure with Local Seismicity, Okataina Volcanic Centre, Taupo Volcanic Zone, Using Double-Difference Seismic Tomography.” *Journal of Volcanology and Geothermal Research* 431 (November): 107653. https://doi.org/10.1016/j.jvolgeores.2022.107653.

Castellanos, Jorge C., Eugene Humphreys, and Robert W. Clayton. 2022. “Evidence of Mantle-Based Deformation Across the Western United States.” *Geophysical Research Letters* 49 (4): e2021GL094854. https://doi.org/10.1029/2021GL094854.

Chai, Chengping, Charles J. Ammon, Monica Maceira, and Robert Herrmann. 2022. “Crust and Upper Mantle Structure Beneath the Eastern United States.” *Geochemistry Geophysics Geosystems* 23 (3): e2021GC010233. https://doi.org/10.1029/2021GC010233.

Christiansen, R. L., G. R. Foulger, and J. R. Evans. 2002. “Upper-Mantle Origin of the Yellowstone Hotspot.” *Geological Society of America Bulletin* 114 (10): 1245–56. https://doi.org/10.1130/0016-7606(2002)114<1245:UMOOTY>2.0.CO;2.

Coblentz, D., and K. E. Karlstrom. 2011. “Tectonic Geomorphometrics of the Western United States: Speculations on the Surface Expression of Upper Mantle Processes.” *Geochemistry Geophysics Geosystems* 12 (November): Q11002. https://doi.org/10.1029/2011GC003579.

Darold, Amberlee, and Eugene Humphreys. 2013. “Upper Mantle Seismic Structure beneath the Pacific Northwest: A Plume-Triggered Delamination Origin for the Columbia River Flood Basalt Eruptions.” *Earth and Planetary Science Letters* 365 (March): 232–42. https://doi.org/10.1016/j.epsl.2013.01.024.

Dueker, K. G., and A. F. Sheehan. 1997. “Mantle Discontinuity Structure from Midpoint Stacks of Converted P to S Waves across the Yellowstone Hotspot Track.” *Journal of Geophysical Research-Solid Earth* 102 (B4): 8313–27. https://doi.org/10.1029/96JB03857.

Eagar, Kevin C., Matthew J. Fouch, and David E. James. 2010. “Receiver Function Imaging of Upper Mantle Complexity beneath the Pacific Northwest, United States.” *Earth and Planetary Science Letters* 297 (1): 141–53. https://doi.org/10.1016/j.epsl.2010.06.015.

Farrell, J., R. B. Smith, S. Husen, and T. Diehl (2014), Tomography from 26 years of seismicity revealing that the spatial extent of the Yellowstone crustal magma reservoir extends well beyond the Yellowstone caldera, Geophys. Res. Lett., 41, 3068–3073.

Huang, Hsin-Hua, Fan-Chi Lin, Brandon Schmandt, Jamie Farrell, Robert B. Smith, and Victor C. Tsai. 2015. “The Yellowstone Magmatic System from the Mantle Plume to the Upper Crust.” *Science* 348 (6236): 773–76. https://doi.org/10.1126/science.aaa5648.

Humphreys, Ed, and Kg Dueker. 1994. “Western United-States Upper-Mantle Structure.” *Journal of Geophysical Research-Solid Earth* 99 (B5): 9615–34. https://doi.org/10.1029/93JB01724.

Iyer, H. M. 1984. “A Review of Crust and Upper Mantle Structure Studies of the Snake River Plain-Yellowstone Volcanic System: A Major Lithospheric Anomaly in the Western U.S.A.” *Tectonophysics*, Lithosphere: Structure, Dynamics and Evolution, 105 (1): 291–308. https://doi.org/10.1016/0040-1951(84)90209-9.

Kasbohm, Jennifer, and Blair Schoene. 2018. “Rapid Eruption of the Columbia River Flood Basalt and Correlation with the Mid-Miocene Climate Optimum.” *Science Advances* 4 (9): eaat8223. https://doi.org/10.1126/sciadv.aat8223.

Lin, Fan-Chi, Michael H. Ritzwoller, Yingjie Yang, Morgan P. Moschetti, and Matthew J. Fouch. 2011. “Complex and Variable Crustal and Uppermost Mantle Seismic Anisotropy in the Western United States.” *Nature Geoscience* 4 (1): 55–61. https://doi.org/10.1038/NGEO1036.

Lü, Ziqiang, Jianshe Lei, Lihong Zhao, Xiang Fu, Jianping Chen, Guanghe Li, and Qinghan Kong. 2021. “Crustal Deformation of Intermontane Basins beneath Central Tien Shan Revealed by Full-Wave Ambient Noise Tomography.” *Tectonophysics* 821 (December): 229143. https://doi.org/10.1016/j.tecto.2021.229143.

Maggi, Alessia, Eric Debayle, Keith Priestley, and Guilhem Barruol. 2006. “Azimuthal Anisotropy of the Pacific Region.” *Earth and Planetary Science Letters* 250 (1): 53–71. https://doi.org/10.1016/j.epsl.2006.07.010.

Montagner, J. -P., G. Burgos, Y. Capdeville, E. Beucler, and A. Mocquet. 2021. “The Mantle Transition Zone Dynamics as Revealed through Seismic Anisotropy.” *Tectonophysics* 821 (December): 229133. https://doi.org/10.1016/j.tecto.2021.229133.

Moschetti, M. P., M. H. Ritzwoller, F. Lin, and Y. Yang. 2010. “Seismic Evidence for Widespread Western-US Deep-Crustal Deformation Caused by Extension.” *Nature* 464 (7290): 885-U94. https://doi.org/10.1038/nature08951.

Nettles, Meredith, and Adam M. Dziewonski. 2008. “Radially Anisotropic Shear Velocity Structure of the Upper Mantle Globally and beneath North America.” *Journal of Geophysical Research-Solid Earth* 113 (B2): B02303. https://doi.org/10.1029/2006JB004819.

Niday, William, and Eugene Humphreys. 2020. “Complex Upper Mantle Anisotropy in the Pacific Northwest: Evidence from SKS Splitting.” *Earth and Planetary Science Letters* 540 (June): 116264. https://doi.org/10.1016/j.epsl.2020.116264.

Savage, M. K. 1999. “Seismic Anisotropy and Mantle Deformation: What Have We Learned from Shear Wave Splitting?” *Reviews of Geophysics* 37 (1): 65–106. https://doi.org/10.1029/98RG02075.

Schmandt, Brandon, Chengxin Jiang, and Jamie Farrell. 2019. “Seismic Perspectives from the Western U.S. on Magma Reservoirs Underlying Large Silicic Calderas.” *Journal of Volcanology and Geothermal Research* 384 (October): 158–78. https://doi.org/10.1016/j.jvolgeores.2019.07.015.

Shen, Weisen, and Michael H. Ritzwoller. 2016. “Crustal and Uppermost Mantle Structure beneath the United States.” *Journal of Geophysical Research-Solid Earth* 121 (6): 4306–42. https://doi.org/10.1002/2016JB012887.

Smith, Rb, and Lw Braile. 1994. “The Yellowstone Hotspot.” *Journal of Volcanology and Geothermal Research* 61 (3–4): 121–87. https://doi.org/10.1016/0377-0273(94)90002-7.

Smith, Robert B., Michael Jordan, Bernhard Steinberger, Christine M. Puskas, Jamie Farrell, Gregory P. Waite, Stephan Husen, Wu-Lung Chang, and Richard O’Connell. 2009. “Geodynamics of the Yellowstone Hotspot and Mantle Plume: Seismic and GPS Imaging, Kinematics, and Mantle Flow.” *Journal of Volcanology and Geothermal Research*, The Track of the Yellowstone Hotspot, 188 (1): 26–56. https://doi.org/10.1016/j.jvolgeores.2009.08.020.

Park, J., and V. Levin (2016), Anisotropic shear zones revealed by back-azimuthal harmonics of teleseismic receiver functions, Geophys. J. Int., 207, 1216-1243.

Tian, You, and Dapeng Zhao. 2012. “P-Wave Tomography of the Western United States: Insight into the Yellowstone Hotspot and the Juan de Fuca Slab.” *Physics of the Earth and Planetary Interiors* 200–201 (June): 72–84. https://doi.org/10.1016/j.pepi.2012.04.004.

vanderLee, S., and G. Nolet. 1997. “Upper Mantle S Velocity Structure of North America.” *Journal of Geophysical Research-Solid Earth* 102 (B10): 22815–38. https://doi.org/10.1029/97JB01168.

Wang, Wanying, and Thorsten W. Becker. 2019. “Upper Mantle Seismic Anisotropy as a Constraint for Mantle Flow and Continental Dynamics of the North American Plate.” *Earth and Planetary Science Letters* 514 (May): 143–55. https://doi.org/10.1016/j.epsl.2019.03.019.

Wang, Xinyang, Dapeng Zhao, Shaohong Xia, and Jiabiao Li. 2022. “Mantle Structure and Flow beneath the Central-Western US: Constraints from Anisotropic Tomography.” *Tectonophysics* 822 (January): 229180. https://doi.org/10.1016/j.tecto.2021.229180.

Wu, Jonny, Yi-An Lin, Nicolas Flament, Jeremy Tsung-Jui Wu, and Yiduo Liu. 2022. “Northwest Pacific-Izanagi Plate Tectonics since Cretaceous Times from Western Pacific Mantle Structure.” *Earth and Planetary Science Letters* 583 (April): 117445. https://doi.org/10.1016/j.epsl.2022.117445.

Zhao, Dapeng. 2021. “Seismic Imaging of Northwest Pacific and East Asia: New Insight into Volcanism, Seismogenesis and Geodynamics.” *Earth-Science Reviews* 214 (March): 103507. https://doi.org/10.1016/j.earscirev.2021.103507.

Zhou, Quan, Jiashun Hu, Lijun Liu, Thomas Chaparro, Dave R. Stegman, and Manuele Faccenda. 2018. “Western U.S. Seismic Anisotropy Revealing Complex Mantle Dynamics.” *Earth and Planetary Science Letters* 500 (October): 156–67. https://doi.org/10.1016/j.epsl.2018.08.015.

## Appendix A: Average Vertical Coherence and Earthquake Distribution for Each Station

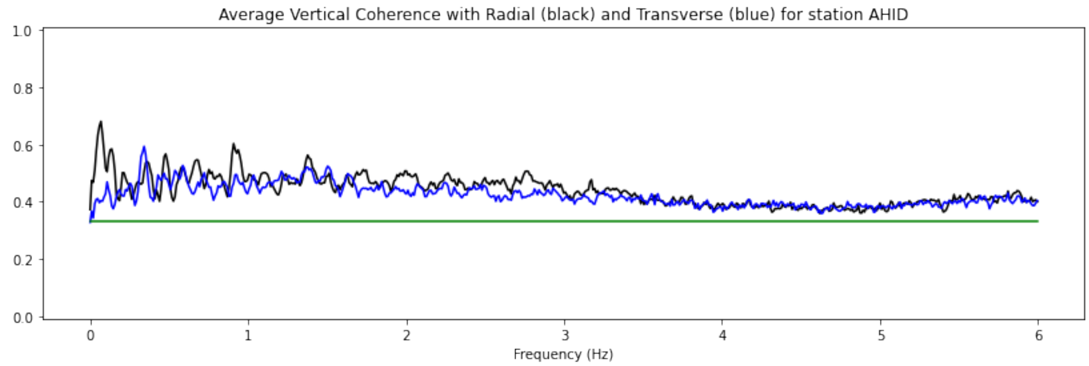


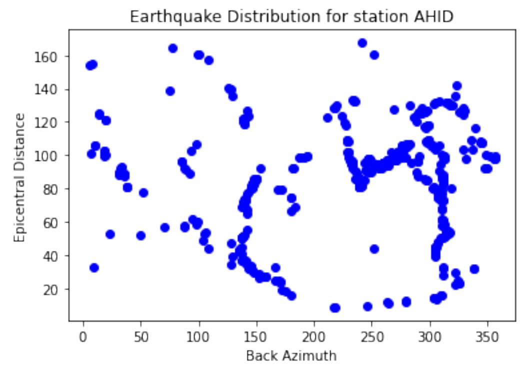


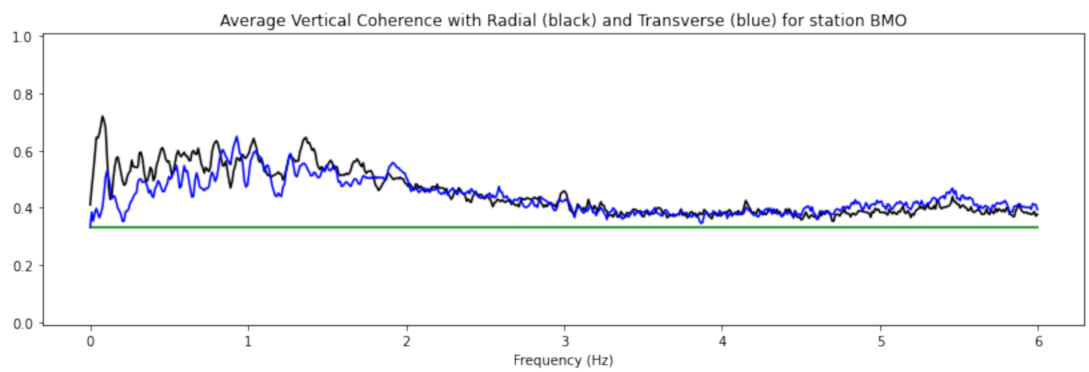


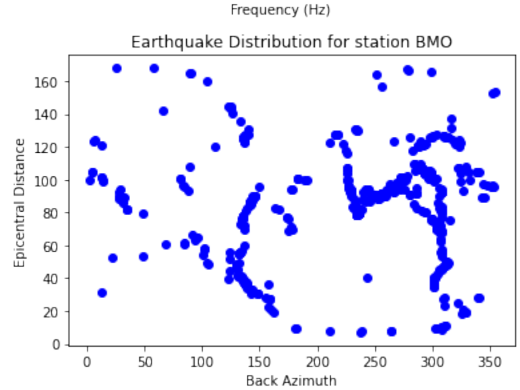

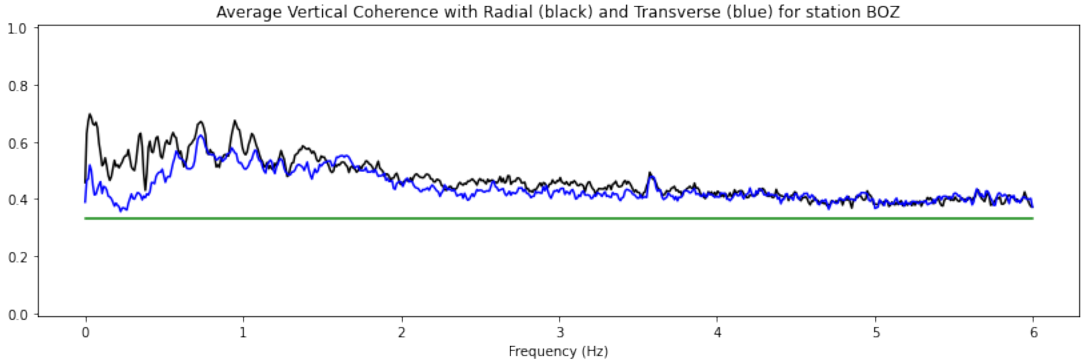
Average Vertical Coherence with Radial (black) and Transverse (blue) for station BOZ
Frequency (Hz)

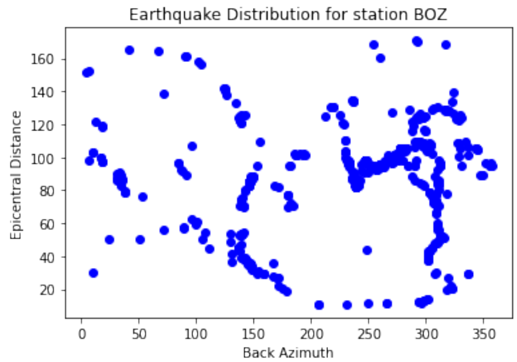
Earthquake Distribution for station BOZ
Epicentral Distance
Back Azimuth

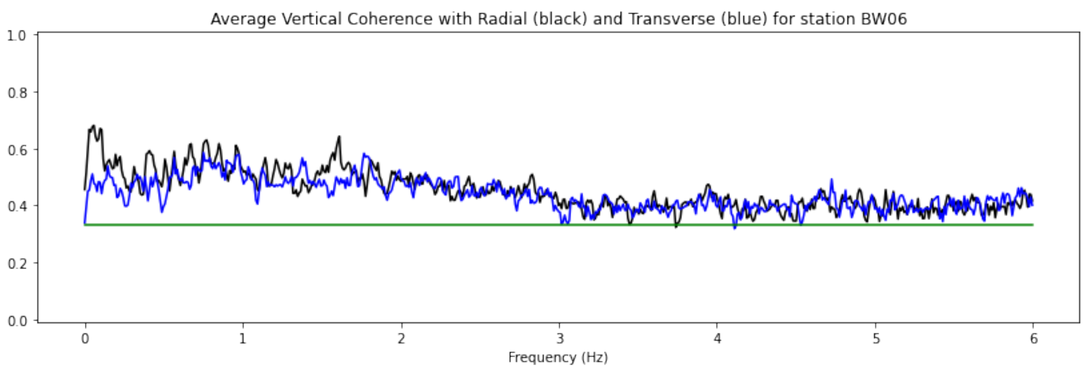
Average Vertical Coherence with Radial (black) and Transverse (blue) for station BW06
Frequency (Hz)

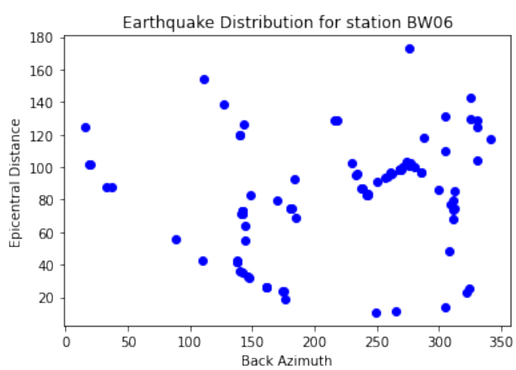
Earthquake Distribution for station BW06
Epicentral Distance
Back Azimuth

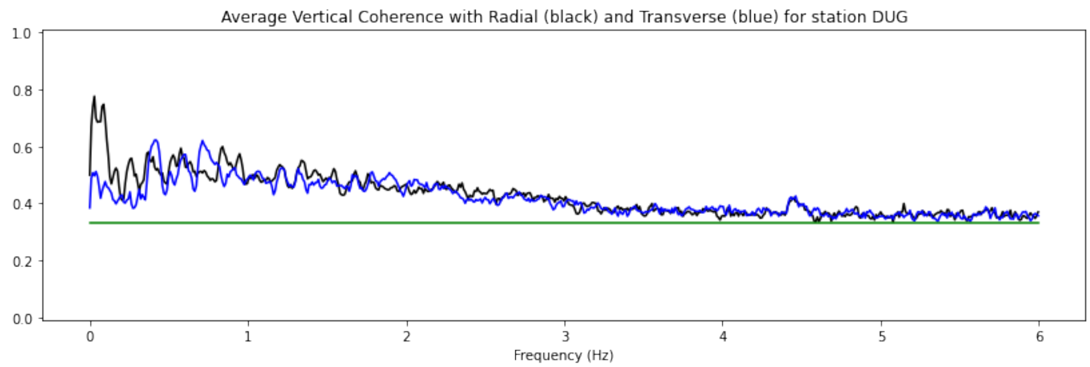
Average Vertical Coherence with Radial (black) and Transverse (blue) for station DUG
Frequency (Hz)

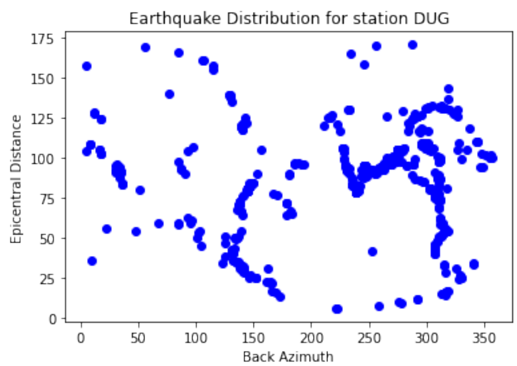
Earthquake Distribution for station DUG
Epicentral Distance
Back Azimuth

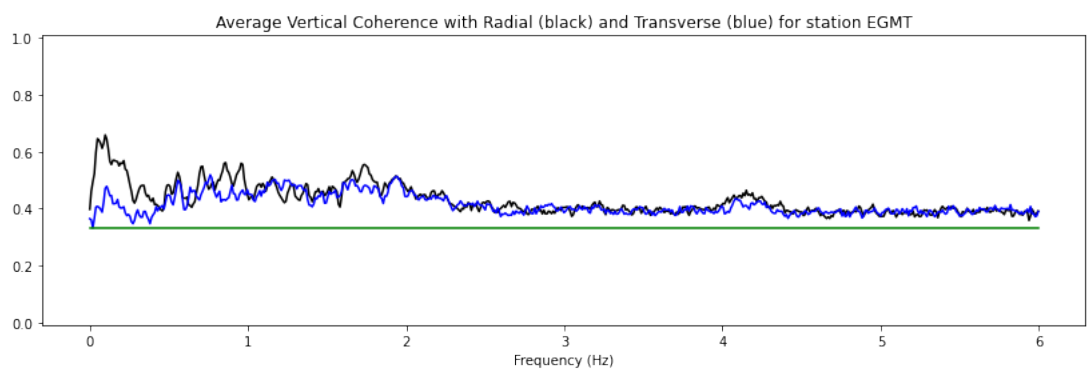
Average Vertical Coherence with Radial (black) and Transverse (blue) for station EGMT
Frequency (Hz)

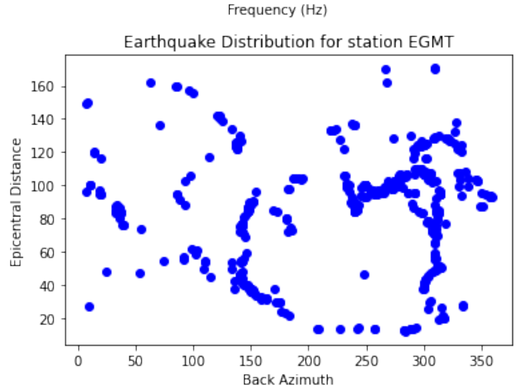
Earthquake Distribution for station EGMT
Epicentral Distance
Back Azimuth

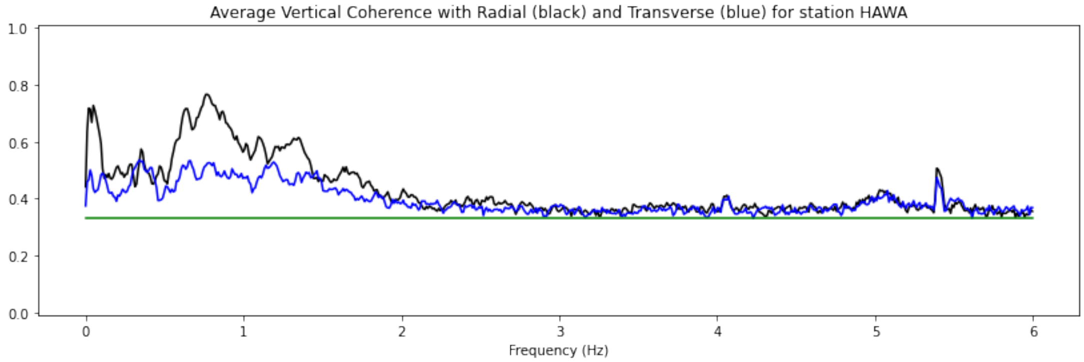
Average Vertical Coherence with Radial (black) and Transverse (blue) for station HAWA
Frequency (Hz)

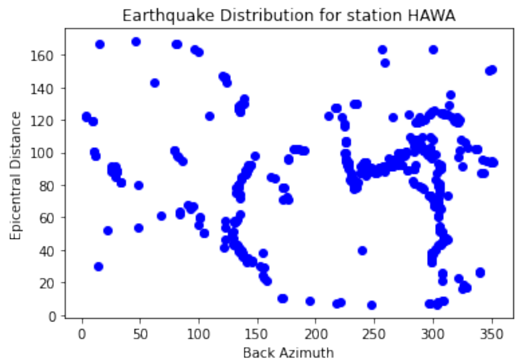
Earthquake Distribution for station HAWA
Epicentral Distance
Back Azimuth

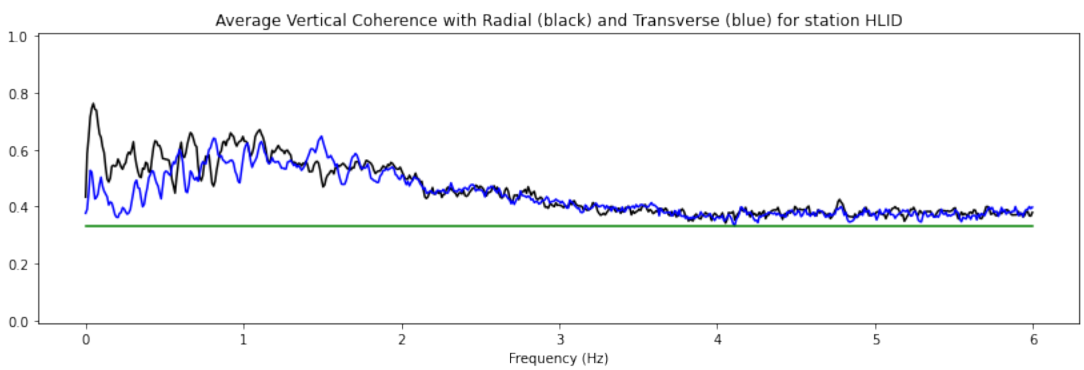
Average Vertical Coherence with Radial (black) and Transverse (blue) for station HLID
Frequency (Hz)

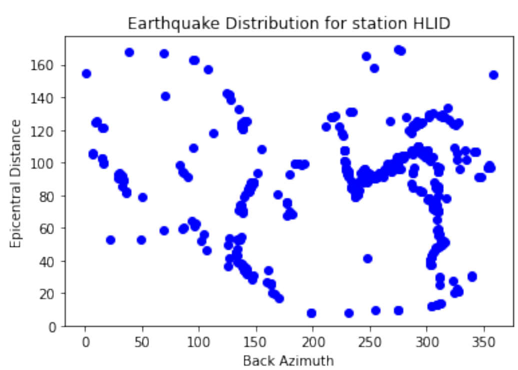
Earthquake Distribution for station HLID
Epicentral Distance
Back Azimuth

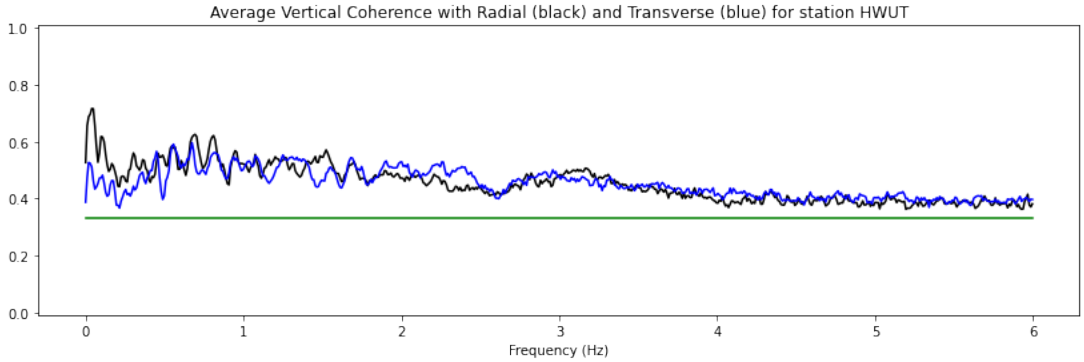
Average Vertical Coherence with Radial (black) and Transverse (blue) for station HWUT
Frequency (Hz)

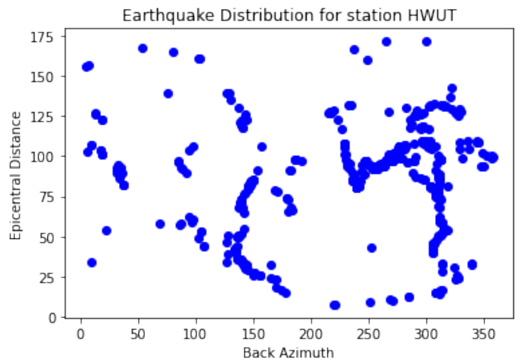
Earthquake Distribution for station HWUT
Epicentral Distance
Back Azimuth

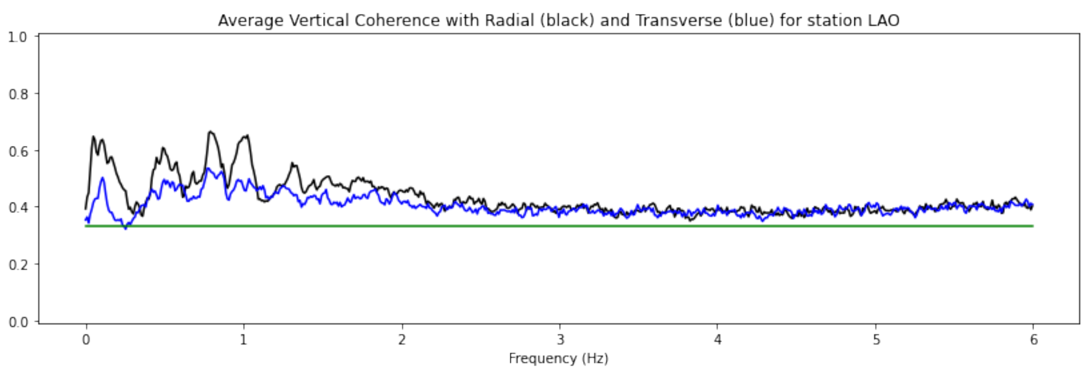
Average Vertical Coherence with Radial (black) and Transverse (blue) for station LAO
Frequency (Hz)

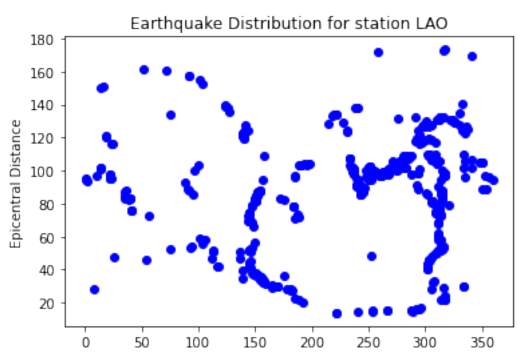
Earthquake Distribution for station LAO
Epicentral Distance
Back Azimuth

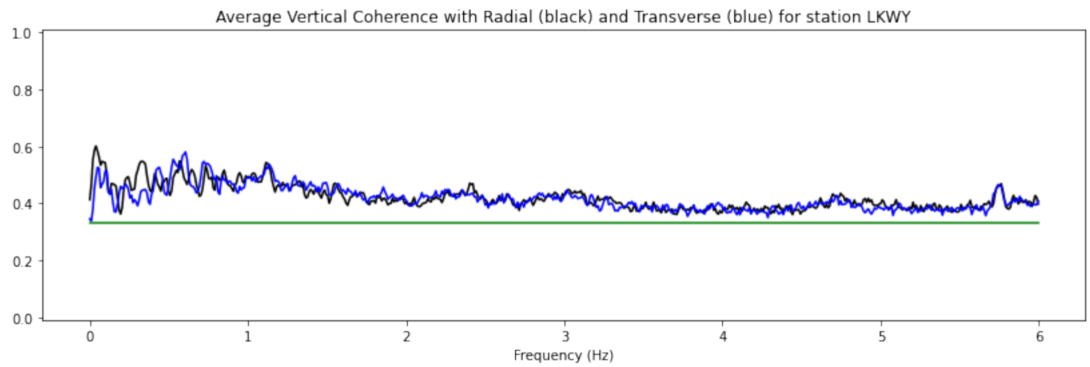
Average Vertical Coherence with Radial (black) and Transverse (blue) for station LKWY
Frequency (Hz)

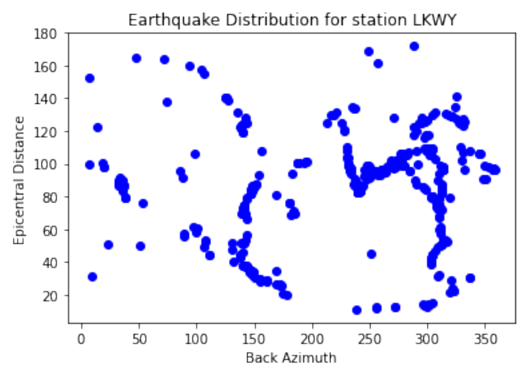
Earthquake Distribution for station LKWY
Epicentral Distance
Back Azimuth

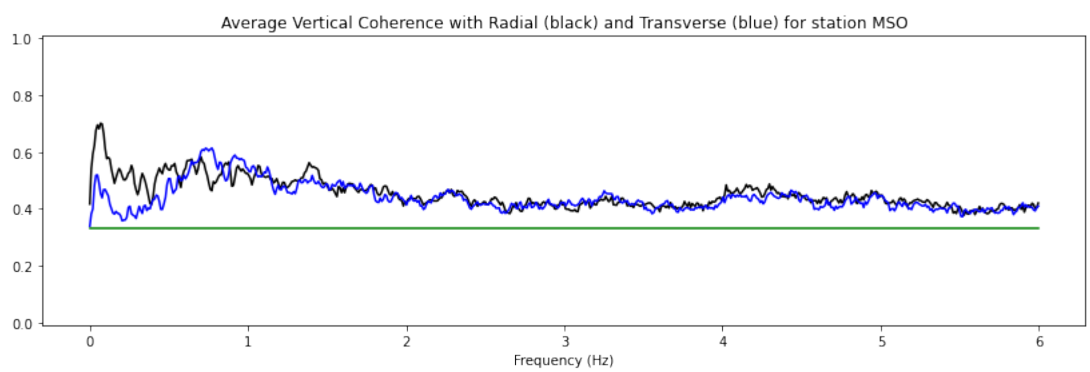
Average Vertical Coherence with Radial (black) and Transverse (blue) for station MSO
Frequency (Hz)

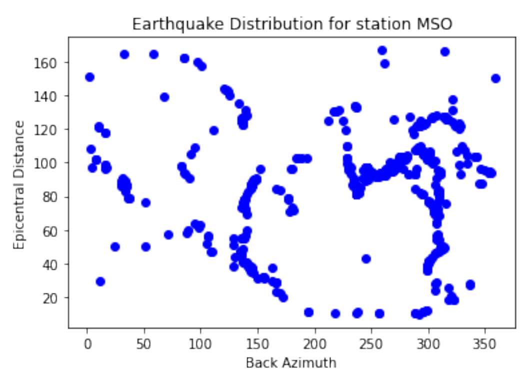
Earthquake Distribution for station MSO
Epicentral Distance
Back Azimuth

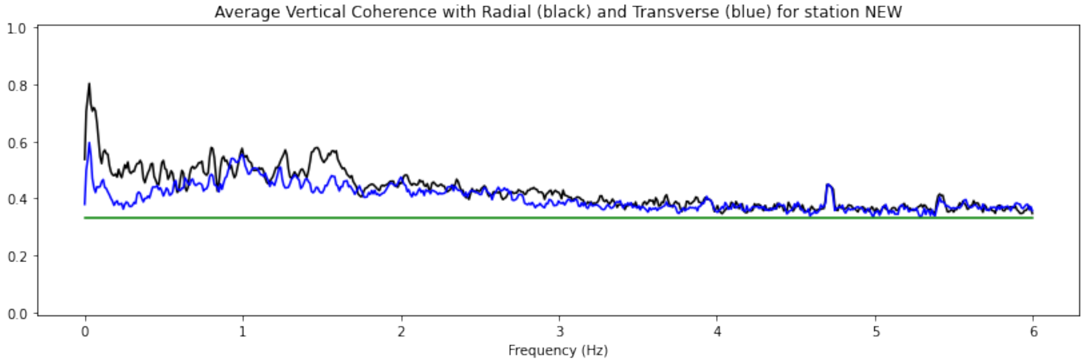
Average Vertical Coherence with Radial (black) and Transverse (blue) for station NEW
Frequency (Hz)

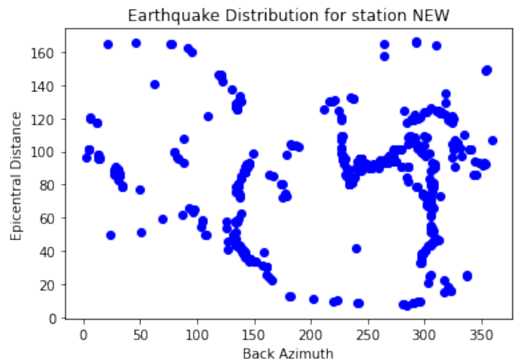
Earthquake Distribution for station NEW
Epicentral Distance
Back Azimuth

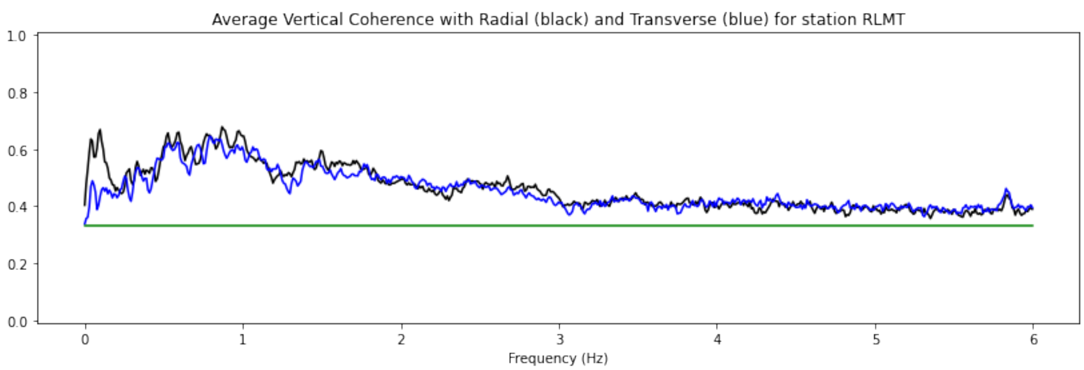
Average Vertical Coherence with Radial (black) and Transverse (blue) for station RLMT
Frequency (Hz)

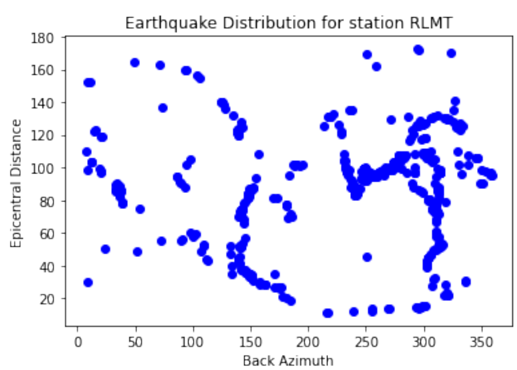
Earthquake Distribution for station RLMT
Epicentral Distance
Back Azimuth

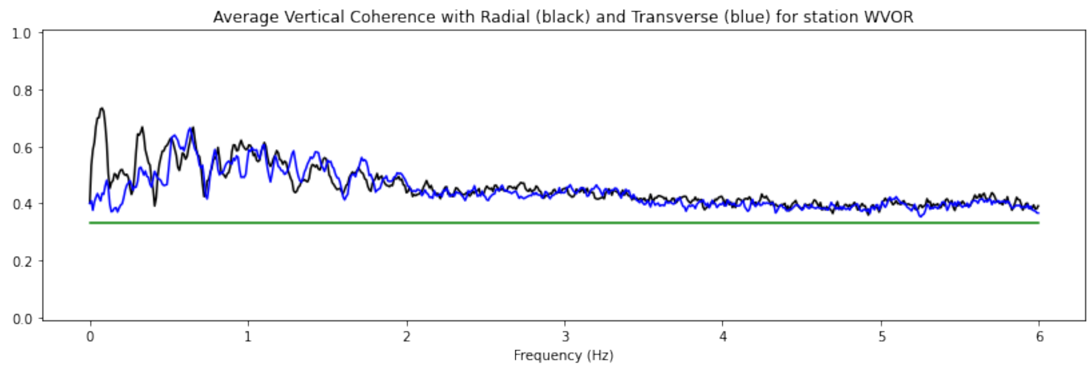
Average Vertical Coherence with Radial (black) and Transverse (blue) for station WVOR
1.0
0.8
0.6
0.4
0.2
0.0
0
1
2
3
4
5
6
Frequency (Hz)

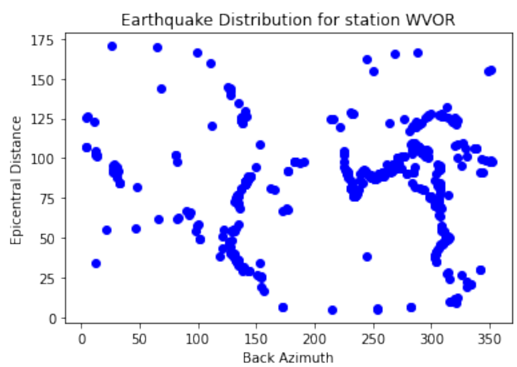
Earthquake Distribution for station WVOR
175
150
125
100
75
50
25
0
Epicentral Distance
0
50
100
150
200
250
300
350
Back Azimuth